



HAL
open science

Time will tell: temporal evolution of Martian gullies and palaeoclimatic implications

T. de Haas, Susan J. Conway, F. E G Butcher, J. Levy, P. Grindrod, T. Goudge, M. R Balme

► **To cite this version:**

T. de Haas, Susan J. Conway, F. E G Butcher, J. Levy, P. Grindrod, et al.. Time will tell: temporal evolution of Martian gullies and palaeoclimatic implications. The Geological Society, London, Special Publications, 2019, 467 (1), pp.165-186. 10.1144/SP467.1 . hal-02270631

HAL Id: hal-02270631

<https://hal.science/hal-02270631>

Submitted on 11 Jan 2021

HAL is a multi-disciplinary open access archive for the deposit and dissemination of scientific research documents, whether they are published or not. The documents may come from teaching and research institutions in France or abroad, or from public or private research centers.

L'archive ouverte pluridisciplinaire **HAL**, est destinée au dépôt et à la diffusion de documents scientifiques de niveau recherche, publiés ou non, émanant des établissements d'enseignement et de recherche français ou étrangers, des laboratoires publics ou privés.

1
2
3
4
5
6
7
8
9
10
11

Time will tell: temporal evolution of Martian gullies and paleoclimatic implications

**T. de Haas^{1,2}, S. J. Conway³, F. E. G. Butcher⁴, J. Levy⁵, P. M. Grindrod^{6,7}, T. A. Goudge⁵,
M. R. Balme⁴**

¹Faculty of Geosciences, Universiteit Utrecht, Utrecht, The Netherlands.

²Department of Geography, Durham University, Durham, UK.

³Laboratoire de Planétologie et Géodynamique, Université de Nantes, Nantes, France.

⁴School of Physical Sciences, The Open University, Milton Keynes, UK.

⁵Jackson School of Geosciences, University of Texas, Austin, USA.

⁶Department of Earth and Planetary Sciences, Birkbeck, University of London, London, UK.

⁷Centre for Planetary Sciences, UCL/Birkbeck, London, UK.

Corresponding author: T. de Haas, t.dehaas@uu.nl

12 **Abstract**

13 To understand Martian paleoclimatic conditions and the role of volatiles therein, the spatio-
14 temporal evolution of gullies must be deciphered. While the spatial distribution of gullies has
15 been extensively studied, their temporal evolution is poorly understood. We show that gully-
16 size is similar in very young and old craters. Gullies on the walls of very young impact craters
17 (< a few Myr) typically cut into bedrock and are free of latitude-dependent mantle (LDM)
18 and glacial deposits, while such deposits become increasingly evident in older craters. These
19 observations suggest that gullies go through obliquity-driven degradation/accumulation cycles
20 over time controlled by (1) LDM emplacement and degradation and by (2) glacial emplace-
21 ment and removal. In glacially-influenced craters the distribution of gullies on crater walls co-
22 incides with the extent of glacial deposits, which suggests that melting of snow and ice played
23 a role in the formation of these gullies. Yet, present-day activity is observed in some gullies
24 on formerly glaciated crater walls. Moreover, in very young craters extensive gullies have formed
25 in the absence of LDM and glacial deposits, showing that gully formation can also be unre-
26 lated to these deposits. The Martian climate varied substantially over time, and the gully-forming
27 mechanisms likely varied accordingly.

1 Introduction

Martian gullies are landforms that consist of an alcove, channel and depositional apron [e.g., *Malin and Edgett, 2000*]. Reconstructing the conditions and processes under which these gullies have formed is key to understanding past climatic conditions on Mars. The formation of gullies has been attributed to (1) water-free sediment flows, either without a volatile [e.g., *Treiman, 2003; Pelletier et al., 2008*] or triggered by sublimation of CO₂ frost [e.g., *Cedillo-Flores et al., 2011; Dundas et al., 2012, 2015; Pilorget and Forget, 2016*] and (2) aqueous debris flows [e.g., *Costard et al., 2002; Levy et al., 2010a; Conway et al., 2011; Johnsson et al., 2014; De Haas et al., 2015a,b*] and fluvial flows (hyperconcentrated or dilute) [e.g., *Heldmann and Mellon, 2004; Heldmann et al., 2005; Dickson et al., 2007; Head et al., 2008; Reiss et al., 2011*]. Each of these formation processes has different implications for Mars' current and recent water-cycle, therefore the presence of habitable environments and resources for future exploration. To better understand the Martian paleoclimate and the role of volatiles therein the spatio-temporal evolution of gullies needs to be understood in detail. While the spatial distribution of gullies has been extensively studied and quantified [e.g., *Heldmann and Mellon, 2004; Balme et al., 2006; Dickson et al., 2007; Kneissl et al., 2010; Harrison et al., 2015*], only few studies have addressed their temporal evolution [e.g., *Dickson et al., 2015; De Haas et al., 2015b*]. When studied, the temporal evolution of gullies has mainly been performed on the basis of local and/or qualitative assessments [*Head et al., 2008; Schon et al., 2009; Raack et al., 2012*]. Yet, for a more detailed temporal understanding quantitative analyses of age constraints and gully size, morphology and morphometry on a global scale are crucial [*Conway and Balme, 2014, 2016; De Haas et al., 2015c*].

Gullies occur in the mid- and high latitudes of Mars, from the poles down to 30° latitudes in the northern and southern hemisphere [e.g., *Heldmann and Mellon, 2004; Balme et al., 2006; Dickson et al., 2007; Kneissl et al., 2010; Harrison et al., 2015*]. The global distribution of gullies corresponds well with the distribution of surface features indicative of past and/or present near-surface ground ice and glacial activity, such as lobate debris aprons (LDA) [*Squyres, 1979*], viscous flow features [*Milliken et al., 2003*] and the latitude dependent mantle (LDM; a smooth, often meters-thick deposit thought to consist of ice with a minor component of dust) [e.g., *Head et al., 2003*]. Gullies are predominantly poleward-facing in the lower midlatitudes, shift to mainly equator-facing at ~45° latitude at both hemispheres and no preferential gully-orientation is found near the poles [*Balme et al., 2006; Kneissl et al., 2010; Harrison et al., 2015*];

60 *Conway, This Issue*]. These observations point towards insolation and atmospheric conditions
61 playing key roles in the formation of Martian gullies.

62 Some authors suggest that gullies predominantly form during glacial periods forced by
63 high orbital obliquity [e.g., *Head et al., 2003, 2008; Dickson and Head, 2009; Dickson et al.,*
64 *2015*], whilst observation of gullies that are morphologically active today have led other au-
65 thors to suggest that gully-formation may have been unrelated to these climatic cycles [e.g.,
66 *Dundas et al., 2010, 2015*]. Gullies are typically recognized as geologically very young fea-
67 tures, owing to a conspicuous absence of superposed impact craters [e.g., *Malin and Edgett,*
68 *2000*], superposition relationships with polygons, dunes and transverse aeolian ridges [e.g., *Ma-*
69 *lin and Edgett, 2000; Reiss et al., 2004*], and their occurrence in young impact craters that formed
70 within the last few million years [*Schon et al., 2009; Johnsson et al., 2014; De Haas et al., 2015c*].
71 *De Haas et al. [2015c]* noted that the size of gullies in relatively pristine host craters is typ-
72 ically similar to the size of gullies found in much older host craters, implying the presence
73 of processes limiting gully growth over time. Gully growth may be limited by: (a) decreas-
74 ing geomorphological activity in gullies over time following crater formation [*De Haas et al.,*
75 *2015c*], (b) the latitude-dependent mantle acting as a barrier to bedrock-incision and enlarge-
76 ment once established [*De Haas et al., 2015c*], (c) alternating erosional/depositional episodes
77 driven by orbital cycles [*Dickson et al., 2015*] or (d) a combination of these factors. Addition-
78 ally, we know that some gully-fans are fed by alcoves that cut into bedrock [e.g., *Johnsson*
79 *et al., 2014; De Haas et al., 2015c; Núñez et al., 2016*] while other gully-fans are fed by al-
80 coves cutting into LDM or glacial deposits [e.g., *Head et al., 2008; Conway and Balme, 2014;*
81 *Núñez et al., 2016*], which may be related to the evolution of the host-crater wall over time.
82 The exact temporal evolution and associated formative mechanisms of gullies, however, re-
83 main to be determined.

84 Here we aim to quantitatively constrain the temporal evolution of Martian gullies. More
85 specifically, we aim to (1) investigate how time and associated climatic variations have affected
86 gullies, (2) provide a conceptual model for the temporal evolution of gullies and (3) deduce
87 paleoclimatic and paleohydrologic conditions from the inferred temporal evolution of gullies.

88 This paper is organized as follows. We first detail study sites, materials and methods.
89 Then we describe the morphology of the gullies and associated landforms in the studied craters,
90 determine gully-size and host crater age, and infer trends of gully morphology and size ver-
91 sus host crater age. Subsequently, we present a conceptual model for the temporal evolution

92 of gullies. Thereafter, we place the relation between gully morphology and associated land-
93 forms and host crater age in an obliquity framework. Next, we draw paleoclimatic implica-
94 tions based on the results presented here. We end with a brief discussion on the potential spa-
95 tial variations on the temporal trends inferred in this paper.

96 **2 Materials and methods**

97 We compare the size of gullies in 19 craters, of which 17 are spread over the southern
98 midlatitudes and 2 occur in the northern midlatitudes (Fig. 1, Table 1). These study sites were
99 selected based on the following criteria: (1) the presence of gullies, (2) the presence of a high-
100 resolution digital terrain model (DTM) made from High Resolution Science Imaging Exper-
101 iment (HiRISE) [McEwen *et al.*, 2007] stereo images (~ 1 m spatial resolution) or the pres-
102 ence of suitable stereo images to produce a DTM ourselves, and (3) a well-defined ejecta blan-
103 ket that has not undergone major resurfacing events since emplacement. The latter enables dat-
104 ing of the ejecta blanket of the crater hosting the gullies, and thereby constraining the earli-
105 est possible start point and thus the maximum duration of gully activity.

106 The dataset comprises all publicly available HiRISE DTMs showing gullies for which
107 dating of the host crater was possible (as of 1 March 2016). Moreover, additional HiRISE DTMs
108 that were previously made by the authors were added to the dataset (Table 2). These DTMs
109 were produced with the software packages ISIS3 and SocetSet following the workflow described
110 by Kirk *et al.* [cf. 2008] (DTM credit Open University or Birkbeck University of London in
111 Table 2) or with the Ames Stereo Pipeline [cf. Broxton and Edwards, 2008; Beyer *et al.*, 2014;
112 Shean *et al.*, 2016] (DTM credit University of Texas in Table 2). Vertical precision of the DTMs
113 is estimated as: $\text{maximum resolution}/5/\tan(\text{convergence angle})$ [cf. Kirk *et al.*, 2008]. Verti-
114 cal precision is generally below 0.5 m and therefore much smaller than the typical depth of
115 the alcoves and the errors associated to vertical DTM precision are therefore negligible com-
116 pared to the measurements we present here.

117 For craters that were already dated in other studies we used the ages reported from the
118 literature (Table 1) [Dickson *et al.*, 2009; Schon *et al.*, 2009; Jones *et al.*, 2011; Johnsson *et al.*,
119 2014; De Haas *et al.*, 2015c; Viola *et al.*, 2015]. The other craters were dated based on the size-
120 frequency distribution of impact craters superposed on the ejecta blanket and rim of the craters
121 using images from the Mars Reconnaissance Orbiter Context Camera (CTX). We defined crater
122 ages based on the crater-size-frequency distribution using the chronology model of Hartmann

123 *and Neukum* [2001] and the production function of *Ivanov* [2001]. Crater counts were performed
124 using Crater Tools 2.1 [*Kneissl et al.*, 2011], crater-size-frequency statistics were analyzed with
125 Crater Stats 2 [*Michael and Neukum*, 2010]. The diameter range used for the age fits was cho-
126 sen so as to include as many of the relatively large craters as possible, and to include as many
127 diameter bins as possible, so as to optimize the statistics. We acknowledge that dating impact
128 craters is delicate: the areas of their ejecta blankets can be small, so the number of (especially
129 relatively large) superposed impact craters is generally restricted, and also the number of small
130 craters may be underestimated due to erosion. Therefore, we maintain a large uncertainty range
131 on the crater ages and stress that the reported host crater ages should be interpreted as a range
132 rather than an absolute value (Table 1, Fig. A.1). Most importantly, we explicitly incorporate
133 the age uncertainty range in all analyses, highlighting that the results presented here are in-
134 sensitive to the age uncertainties.

135 We use alcove-size as a measure of gully maturity, and compare the size of the gully-
136 alcoves in the study craters using their volume and mean depth (alcove volume divided by al-
137 cove area). Gully-alcoves do not exclusively form by the dominant gully-forming mechanism,
138 but are expected to grow in size over time, given persistent gully-forming processes, so that
139 alcove-size provides a proxy for gully maturity. The growth rate of gully-alcoves probably de-
140 creases exponentially over time [*De Haas et al.*, 2015c]. Following crater formation, initial al-
141 coves may form by landsliding such that initial rates of alcove weathering, erosion and en-
142 largement are probably large due to the initially highly fractured, oversteepened, and unsta-
143 ble crater wall [e.g., *Kumar et al.*, 2010; *De Haas et al.*, 2015c]. Over time, the crater wall sta-
144 bilizes and alcove growth rates will decrease towards more stable and lower background rates.
145 Landsliding and dry rockfalls are expected to contribute to initial gully-growth, but as gullies
146 mature and their alcove gradients decrease, rockfalls will accumulate within alcoves; the gully-
147 forming mechanism is needed to evacuate this debris from the alcoves and to enable further
148 gully growth. *De Haas et al.* [2015c] show that gully-alcoves are substantially larger than non-
149 gullied alcoves (gully-alcoves are larger by a factor 2-60 in Galap, Istok and Gasa craters), im-
150 plying that a large part of alcove enlargement can be attributed to gully-forming processes, and
151 that gully-alcove size can be used as a proxy for gully maturity. Furthermore, apart from size
152 differences, alcove slopes and drainage patterns also differ substantially between gullied and
153 non-gullied alcoves [e.g., *Conway*, 2010; *Conway et al.*, 2011, 2015].

154 The volume of material eroded from the alcoves was determined from the elevation mod-
155 els assuming that the ridges surrounding the alcoves (i.e., the alcove watershed) represent the

156 initial pre-gully surface [cf. *Conway and Balme, 2014; De Haas et al., 2015a,c*]. Alcove vol-
157 ume was then derived by subtracting the original from the pre-gully surface. Such volume es-
158 timates are probably conservative, as the volumes are likely to be underestimated as most of
159 the ridges that define the alcove have probably also experienced erosion. In addition, small
160 geometrical errors may arise from digitizing alcove-ridges: error propagation calculations by
161 *Conway and Balme* [2014] suggest that such alcove volume estimates are accurate within 15%.
162 The errors associated with estimating alcove volumes are, however, much smaller than the intra-
163 and inter-crater alcove size variability and therefore do not influence our results.

164 We categorized craters according to the presence or absence of morphological evidence
165 for (1) present or past glaciation [e.g., *Arfstrom and Hartmann, 2005; Head et al., 2008; Levy*
166 *et al., 2009; Head et al., 2010; Hubbard et al., 2011*] and (2) mantling by the LDM [e.g., *Mus-*
167 *tard et al., 2001*] (Fig. 2). We identified evidence of past or present glaciation on the walls and
168 floors of craters according to the criteria described by *Head et al.* [2010] and *Levy et al.* [2010b]
169 for lobate debris aprons and concentric crater fill (CCF) (Fig. 2a-b). These criteria include:
170 longitudinal and transverse ridges, troughs and fractures arising from flow deformation and
171 failure of debris-covered ice [*Berman et al., 2005, 2009; Levy et al., 2010b*]; spatulate depres-
172 sions at the margins of crater floor-filling materials [*Head et al., 2008*]; downslope-oriented
173 horseshoe-shaped lobes arising from flow around isolated topographic obstacles; and circu-
174 lar to elongate pits indicative of sublimation of debris-covered ice [*Head et al., 2010*]. We also
175 classified craters as glaciated if arcuate ridges with similar geometries to those interpreted by
176 *Arfstrom and Hartmann* [2005] and *Hubbard et al.* [2011] as terminal moraines, were present.

177 We classified craters as containing LDM deposits if meter-to-kilometer-scale topogra-
178 phy appeared to be softened by a thin (~1-10m) drape of smooth or polygonized material [e.g.,
179 *Mustard et al., 2001; Kreslavsky and Head, 2002; Levy et al., 2009*] that obscured the under-
180 lying fractured bedrock (Fig. 2c-f). We categorized craters as such regardless of the stratigraphic
181 relationship between LDM deposits and the gullies. In some cases, LDM materials partially
182 or completely infilled gully alcoves and other topographic depressions (e.g. small impact craters
183 within the host crater) [e.g., *Christensen, 2003*]. In other cases, gullies incised into LDM de-
184 posits [e.g., *Milliken et al., 2003; Conway and Balme, 2014*]. We classified craters as devoid
185 of LDM if pristine gully alcoves were clearly incised into exposed fractured bedrock with no
186 evidence of incision into, or infilling by, a mantling layer. Such alcoves may have been for-
187 merly covered by LDM deposits that have subsequently been removed, but have clearly cut
188 substantially into bedrock material and all remnants of LDM are currently gone.

189 3 Results

190 3.1 Morphology

191 In this section the morphology of gullies within the studied craters is divided into three
 192 categories, based on their association with LDM and glacial deposits. We describe the mor-
 193 phology of the landforms in the study craters per category. The three morphological categories
 194 of landform assemblages we distinguish are: (1) gullies free of LDM and glacial deposits, (2)
 195 gullies notably influenced by LDM in the absence of glacial deposits and (3) gullies in asso-
 196 ciation with LDM and glacial deposits. Below we describe the morphology of these types of
 197 gully systems in more detail, and divide the studied craters into one of the three categories.

198 Istok, Gasa and Galap crater contain gullies that are free of LDM and glacial deposits,
 199 and which cut directly into the original crater-wall material (Fig. 3) [*Schon et al.*, 2012; *Johns-*
 200 *son et al.*, 2014; *De Haas et al.*, 2015a,b]. These craters host large gully systems on their pole-
 201 facing, northern, walls. The largest alcoves are located in the middle of the pole-facing slope
 202 and alcoves become progressively smaller in clockwise and counter-clockwise directions. The
 203 alcoves have a crenulated shape, indicating headward erosion into the crater rim, and are gen-
 204 erally complex, consisting of multiple sub-alcoves. The sharp divides between the alcoves and
 205 the upper rims often expose fractured bedrock material, which appears to be highly brecciated
 206 and contains many boulders. The alcoves have a very pristine appearance, suggesting that all
 207 alcoves have been active recently and there has been little or no infill by secondary processes.
 208 The absence of LDM deposits in the gullies is demonstrated by the presence of highly brec-
 209 ciated alcoves hosting many boulders, solely exposing bedrock, the abundance of meter-sized
 210 boulders on the depositional fans and the lack of landforms associated with the LDM such as
 211 polygonally patterned ground. This does not completely rule out the possibility that these al-
 212 coves were formerly covered by LDM deposits that have now been removed, but we would
 213 expect in that case remnants of LDM to be recognizable in places. As such, we favor a for-
 214 mation mechanism unrelated to LDM deposits for these gully-systems.

215 Roseau, Domoni, Tivat and Raga crater encompass gullies that have interacted with and
 216 have been influenced by LDM deposits (Fig. 4). Tivat and Raga are small craters (Table 1)
 217 and have poorly developed gullies. Tivat contains a single and Raga a few, small-sized, gully
 218 systems with elongated alcoves that are sometimes v-shaped in cross-section (Fig. 4). The craters
 219 seem covered by a smooth drape of LDM, as shown by the softened appearance of multiple
 220 small craters and the presence of patterned ground covering parts of the crater including al-

221 cove walls. The v-shaped cross-section of many of the gully-alcoves suggests that these al-
222 coves have formed into older mantling material [cf. *Aston et al.*, 2011]. Roseau crater contains
223 well-developed gullies on its pole-facing walls. The gully-alcoves as well as the gully-fan de-
224 posits are covered by a smooth drape of LDM material, as implied by the softened appear-
225 ance of these deposits. All gullies in Roseau crater seem to be covered by LDM material to
226 a similar degree. Domoni crater contains gullies on all crater slopes so there is no preferen-
227 tial gully orientation in this crater. Some gullies in this crater have a fresh appearance, with
228 brecciated alcoves hosting many boulders cutting directly into the original crater-rim material,
229 whereas other neighboring gullies are covered by mantling material (Fig. 4b). This suggests
230 that the gullies in Domoni crater have at least experienced one episode of gully formation (ini-
231 tially unrelated to the LDM), followed by LDM covering and subsequently reactivation of some
232 of the gullies, thereby eroding and removing the LDM from the catchments. This is further
233 supported by the presence of gully-fan lobe surfaces that show different degrees of modifica-
234 tion, where the superposed lobes are always the most pristine. The present-day alcoves in Roseau
235 crater and Domoni crater, both those with and without LDM cover, cut directly into the crater
236 rim. Despite the abundance of LDM deposits in Roseau, Domoni, Tivat and Raga crater there
237 is no morphological evidence for the presence of glacial landforms.

238 The other studied craters show evidence for one or multiple episodes of glaciation (Talu,
239 Flateyri, Taltal, Moni, Artik, Hale, Corozal, Palikir, Nqulu, Langtang, Lyot and Bunnik crater)
240 followed by gully formation (Figs 5, 6). The gullies in these craters are often, at least partly,
241 covered by LDM deposits. There is evidence of substantial ice accumulation having occurred
242 in the past on the crater walls that now host the gullies. This evidence comes in the form of
243 arcuate ridges interpreted as moraine deposits, hummocky deposits from sublimation till re-
244 maining from the sublimation and downwasting of glacial ice containing debris, and ridges
245 following the viscous flow patterns of debris-covered glaciers on Mars [cf. *Head et al.*, 2008,
246 2010]. Although these landforms are located on the lower and shallower slopes of the crater
247 they cannot have formed via glacial processes without the presence of large bodies of ice on
248 the steeper, higher, slopes above. The distribution of the gullies within the craters coincides
249 with the inferred glacial extent. Additionally, the gullies that form in the hollows of formerly
250 glaciated crater walls do not extend up to the crater rim and are often elongated to v-shaped,
251 suggesting incision into ice-rich, unlithified, sediments [*Aston et al.*, 2011]. The gullies super-
252 pose and postdate the glacial deposits, and thus formed following recession of the glaciers.
253 In some craters the tops of former alcoves are still visible on the crater wall.

254 A typical example of this can be found in Langtang crater (Fig. 5). These alcoves are
255 likely the remnants of former gully alcoves, which may have been excavated and enlarged by
256 glacial activity [cf. *Arfstrom and Hartmann, 2005*]. Glacier(s) may have formed within the old
257 gully alcoves, thereby creating a broader glacial alcove and enlarging the former gully alcove,
258 potentially explaining the relatively broad and smooth appearance of the alcoves. The extent
259 of sublimation-till deposits provides evidence for a major episode of glaciation in Langtang
260 crater, whereas moraine deposits define the extent of a younger, smaller, glacial episode (Fig. 5).
261 The pitted lobate sublimation till deposit which extends ~ 1.5 km across the northern portion
262 of the floor of Langtang crater may be the remnant of an LDA which formed during a ma-
263 jor episode of glaciation. Spatulate depressions with raised rims within this deposit at the base
264 of the crater wall are similar to those interpreted by *Head et al. [2008]* as troughs carved by
265 the more recent invasion of pre-existing deposits on the crater floor by smaller glacial lobes,
266 which advanced down the crater wall and were subsequently removed by sublimation. Along
267 the crater rim the crowns of alcoves that cannot be directly related to gully-fans are visible.
268 Below these alcoves, younger alcoves have cut into the crater wall. These younger alcoves are
269 connected to gully-fans, whereas the fan deposits associated to the older generation of alcoves
270 are not visible anymore. These deposits may have been overridden by younger glaciers that
271 have been present within the crater, although this remains speculative as there is no evidence
272 of glacial deposits superposing older gully deposits apart from the possible remnants of older
273 alcoves.

274 In Bunnik crater there is evidence for at least two different generations of alcoves (stage
275 1 and 2), and potentially for four generations of alcoves (stage 3 and 4) (Fig. 6). These gen-
276 erations can be distinguished based on cross-cutting relationships and degree of degradation.
277 The youngest (stage 1) alcoves have cut up to 25 m deep into a thick layer of LDM deposits
278 that occupy the hollows of older, stage 2, alcoves, demonstrated by their elongated shape and
279 abundance of polygonal patterned ground [*Conway and Balme, 2014*]. In front of the gully-
280 fans, just below the youngest alcoves, a complex of ridges is present, which may mark the ex-
281 tent of former ice accumulation. Below these systems there is a relatively gently sloping apron
282 ($5\text{-}10^\circ$) composed of juxtaposed degraded cone-shaped deposits. These deposits are much younger
283 than the crater floor given the marked difference in abundance of superposed craters. We in-
284 terpret these deposits to be the remnants of large inactive fans given their slope and cone shape.
285 This interpretation is supported by the absence of morphologies indicative of flow deforma-
286 tion or volatile loss [e.g., *Head et al., 2010*], which leads us to exclude a glacial origin for these

287 deposits. These fan deposits might have originated from the large abandoned alcoves of stage
 288 3 and 4.

289 **3.2 Crater age versus and gully size and landform assemblage**

290 The craters studied here range in age from <1 Ma up to multiple billion years (Table 1, Fig.A.1).
 291 Figure 7 shows the relation between host crater age and alcove volume and mean alcove depth
 292 for the active alcoves of the gullies in the craters studied here. The size of the alcoves has a
 293 similar range in all craters regardless of crater age, implying that there is a mechanism that
 294 limits gully size over time. Notably, gullies in even the youngest craters are similar in size to
 295 those present in craters of billions of years old. To explain this, we subdivide the gullies into
 296 the three morphological categories described in the previous section. From this analysis it be-
 297 comes clear that the youngest craters host gullies that are unaffected by LDM or glacial episodes,
 298 whereas the LDM and glacial influence increases with crater age. The oldest crater unaffected
 299 by LDM and glacial deposits is Galap crater (best-fit age 6.5 Ma; 5-9 Ma uncertainty range).
 300 Roseau crater (best-fit age 2.8 Ma; 2-4 Ma uncertainty range) is the youngest crater affected
 301 by LDM deposits, whereas Talu crater (best-fit age 14 Ma; 10-22 Ma uncertainty range) is the
 302 youngest crater in our dataset to have been affected by glaciation. In contrast, the other three
 303 craters within the same age range (~10-50 Ma: Domonik, Tivat and Raga) are affected by LDM
 304 deposits, but not by glaciers. The older craters in our dataset (>50 Ma) have all been affected
 305 by the LDM and glaciation. Moreover, potential evidence for multiple episodes of activity, by
 306 the presence of multiple generations of alcoves is mainly found in the oldest craters (see for
 307 example Figs 5 and 6).

308 Artik crater provides quantitative evidence for very recent gully deposits in a much older
 309 host crater. Artik crater is covered with secondaries from the Gasa crater impact, which pro-
 310 vide a chronological marker event inside Artik crater at ~1.25 Ma (Fig. 8) [*Schon et al., 2009;*
 311 *Schon and Head, 2011*]. Gasa crater is located ~100 km to the southwest of Artik crater. The
 312 alcoves of the gullies in Artik crater cut in LDM material as indicated by their elongated shape
 313 [*Schon and Head, 2011*]. The presence of an arcuate ridge in front of the gully-fan suggests
 314 former ice accumulation and potentially glacial activity. The oldest gully-fan lobe of the ma-
 315 jor gully complex is superposed by Gasa secondaries, implying that its formation predates Gasa
 316 impact, whereas the younger gully-fan lobes are free of secondaries and therefore postdate the
 317 formation of Gasa crater [*Schon et al., 2009; De Haas et al., 2013*]. This shows that the gul-

318 lies in Artik crater are less than a few million years old. Artik crater itself formed ~ 590 Ma
319 (uncertainty range 300 Ma - 1 Ga) and is therefore much older than the gullies.

320 **4 Discussion**

321 **4.1 Model of the temporal evolution of gullies**

322 The close association between the distribution of gullies and the extent of former glaciers,
323 the evidence for glacial emplacement and multiple generations of alcoves in some locations,
324 and the crosscutting relations between glacial landforms and gullies suggest an intimate link
325 between glaciation and gully formation in the studied craters, with glaciers potentially remov-
326 ing or burying gully deposits but potentially also providing volatiles for new gully formation
327 after deglaciation. By combining crater age with these observations of gully morphology and
328 associated landform assemblages as discussed here and in literature, we provide the follow-
329 ing conceptual model for the temporal evolution of gullies on Mars (Fig. 9):

330 (1) Following crater formation gullies may develop in midlatitude to polar craters. The
331 mechanism by which these gullies form depends on the climatic conditions during crater for-
332 mation. If obliquity allows snow/ice accumulation in alcoves the gullies may predominantly
333 form by aqueous processes, whereas alternatively they may perhaps predominantly form by
334 dry processes, likely involving CO_2 , during periods where snow/ice does not accumulate or
335 melt. Following crater formation initial rates of geomorphic activity are typically high, because
336 the interior parts of crater rims are generally oversteepened shortly after their formation and
337 consist of highly faulted, fractured and fragmented materials [e.g., *Kumar et al.*, 2010]. As a
338 result they are particularly prone to weathering, enabling rapid growth of alcoves and provid-
339 ing ample sediment to be transported to gully-aprons [‘paracratering’ effect; see *De Haas et al.*,
340 2015c, for a more extensive description of this effect]. Gullies may therefore rapidly form in
341 fresh craters, which may explain the vast gully systems that have formed in Istok and Gasa
342 crater within ~ 1 Myr (Fig. 3).

343 (2) Over time the crater wall stabilizes and as a result geomorphic activity, and thus gully
344 growth, decreases [cf. *De Haas et al.*, 2015c]. If obliquity is high enough for LDM deposi-
345 tion to occur, LDM deposits may accumulate in gully alcoves. When LDM covers gullies, bedrock
346 alcoves are protected from weathering and geomorphic flows will largely result in mobiliza-
347 tion and transport of the clastic material present in the LDM [*De Haas et al.*, 2015b]. Geo-
348 morphic flows will therefore hardly erode the original crater-wall surface or talus slope. As

349 a result, there will be little or no net gully-alcove growth. Evidence for cyclical LDM accumulation-
350 degradation and interactions thereof with gullies have also been observed and described in de-
351 tail by *Dickson et al.* [2015].

352 (3) When mean obliquity is high and local conditions allow sufficient accumulation of
353 snow/ice on the interior wall of an impact crater and in gully-alcoves, glaciers may develop.
354 As glaciers grow and flow down the crater wall, they may override and obscure or remove older
355 deposits on the crater wall and within the crater. Only the upper parts of alcoves (crowns) may
356 generally be preserved on the crater wall (Figs 5, 6), although distal fan deposits may be pre-
357 served when glaciers do not reach far enough downslope (Fig. 6). For the rest, the removal
358 or burial of former gully deposits by glacial activity can only be hypothesized, given the lack
359 of preserved old gully deposits below glacial features.

360 (4) When mean obliquity decreases and the glaciers sublimate and potentially melt, a
361 smoothed crater wall becomes exposed whereon former gully deposits have been largely re-
362 moved or obscured. Deglaciation exposes an oversteepened crater wall, which is likely highly
363 fractured due to enhanced stress relaxation caused by debuttressing (removal of the support
364 of adjacent glacier ice) [e.g., *Ballantyne*, 2002]. Moreover, sublimation or melting of a glacier
365 will leave abundant loose sediment behind, which was formerly within or on top of the glacier
366 ice. This will lead to enhanced geomorphic activity on a crater wall following deglaciation,
367 decreasing to a background rate over time [‘paraglacial’ effect; *Church and Ryder*, 1972]. Gul-
368 lies may thus rapidly form and develop following deglaciation (similar to the enhanced gully
369 growth after crater formation), especially as melt of former glacial ice may cause debris flows
370 and fluvial flows [*Head et al.*, 2008].

371 (5) The gully formation/degradation cycles may repeat themselves (between the above
372 described phases 2 and 4) if time and environmental conditions allow.

373 In short, gullies develop rapidly following crater formation or deglaciation. If time and
374 local conditions permit, they may subsequently go through formation/degradation cycles driven
375 by (1) LDM emplacement and degradation and by (2) glacial emplacement and removal. The
376 former cycles are probably more common, whereas the latter cycles have a stronger effect on
377 the gullies as they may completely remove or bury gully deposits. These cycles limit gully-
378 size and -age, explaining their pristine appearance.

379 4.2 Timing and link to obliquity cycles

380 The current obliquity of Mars is $\sim 25^\circ$ but obliquity has been greater in the past. Dur-
381 ing the last 250 Ma obliquity values likely ranged from 0° to 65° [Laskar *et al.*, 2004]. From
382 21 to 5 Ma obliquity ranged between 25° and 45° around an average obliquity of 35° (Fig. 10),
383 while from 5 Ma to present-day obliquity dropped to a mean of 25° , varying between 15° and
384 35° . These obliquity variations have inevitably had large effects on the Martian climate and
385 water cycle, and have likely caused alternating glacial and interglacial periods in the past [e.g.,
386 Head *et al.*, 2003; Forget *et al.*, 2006].

387 The obliquity threshold for snow and ice transfer to the midlatitudes has been estimated
388 to be 30° [e.g., Head *et al.*, 2003]. The threshold for melting and associated morphological
389 activity is probably higher but unknown [Williams *et al.*, 2009], likely in the 30 - 35° obliquity
390 range [De Haas *et al.*, 2015a]. However, Kreslavsky *et al.* [2008] suggest that an active per-
391 mafrost layer has not been present on Mars in the last ~ 5 Ma when mean obliquity was rel-
392 atively low, because insufficient ground ice was able to melt. Using a global circulation model
393 Madeleine *et al.* [2014] predict annual snow/ice accumulations of ~ 10 cm in the midlatitudes
394 at 35° obliquity. Melting of such quantities of snow would probably be sufficient to cause sub-
395 stantial flows in gullies, especially as snow is being trapped and collected in alcoves [Chris-
396 tiansen, 1998]. It would, however, probably be insufficient for the formation of glaciers, es-
397 pecially as most snow is predicted to sublimate at 35° obliquity [Williams *et al.*, 2009]. Global
398 circulation models show that sufficient amounts of ice may be moved towards the midlatitudes
399 to cause midlatitude glaciation, during transitions from high ~ 40 - 45° to moderate obliquity
400 of 25 - 35° [e.g., Levrard *et al.*, 2007; Madeleine *et al.*, 2009]. High mean obliquity ($\sim 45^\circ$) re-
401 sults in accumulation of tropical mountain glaciers at the expense of polar reservoirs. A sub-
402 sequent transition to moderate ($\sim 35^\circ$) obliquity would increase equatorial insolation, mobi-
403 lize equatorial ice and drive deposition of large volumes of ice in the midlatitudes. In the mid-
404 latitude regions, this ice is likely to accumulate on plateaus and in alcoves and flow down-slope
405 to form glacial systems [e.g., Baker *et al.*, 2010]. Accordingly, Head *et al.* [2008] suggest that
406 higher obliquities led to more water in the atmosphere in the midlatitudes and deposition of
407 snow and ice, particularly in favored and shielded microenvironments such as pole-facing crater
408 interiors at these latitudes.

409 These hypothesized thresholds and models for snow and ice transfer to the midlatitudes,
410 melting and glaciation correspond well with our observations on combined crater age and mor-

411 phology (Fig. 10). The three craters without any evidence for LDM or glaciation formed within
412 the last 5 Ma, and thus fall within the period of relatively low mean obliquity (Istok and Gasa)
413 or at the end of the last high mean obliquity period (Galap). The estimated age of Istok crater
414 is younger than the termination of the most recent mantling episode ~ 0.4 Myr age [Head *et al.*,
415 2003; Smith *et al.*, 2016], explaining the lack of LDM deposits. The timing of the termination
416 of the most recent mantling episode may vary with latitude, however, and may have finished
417 earlier at lower latitudes. Gasa and Galap crater have likely experienced multiple $>30^\circ$ obliq-
418 uity periods, suggesting that LDM deposition may have occurred in these craters given their
419 location within the southern midlatitude band. The apparent absence of LDM deposits in these
420 craters may be because LDM was never deposited in Gasa and Galap craters, which might be
421 possible given their relatively low latitudes of 35.7° S and 37.7° S, respectively. Alternatively,
422 the LDM deposits emplaced in these craters were too thin to be preserved and too thin to sig-
423 nificantly affect gully formation. The age of ~ 2.8 Ma of the youngest crater covered by LDM
424 deposits, Roseau crater (latitude 41.7° S), is consistent with temporal constraints on the lat-
425 est episode of LDM deposition by Schon *et al.* [2012]. The older craters that have all been ex-
426 posed to high mean obliquity for a substantial time period show evidence of LDM accumu-
427 lation and glacial activity. Talu crater is the youngest crater that hosts viscous flow features.
428 Its age of 10-22 Ma suggests that glacial landforms can develop on relatively recent timescales,
429 at least locally, as the other three craters with the same age show evidence for LDM deposi-
430 tion but not for glaciation. The older craters, all 300 Ma or older, show evidence for LDM and
431 glaciation as would be expected because these craters have experienced multiple and long episodes
432 of high obliquity [Laskar *et al.*, 2004].

433 This temporal trend is in good agreement with the inferred timing of glacial activity in
434 the Martian midlatitudes. Dating of glacial landforms, such as lobate debris aprons and lin-
435 eated valley fill, provide evidence for large-scale glacial episodes in the northern and south-
436 ern midlatitudes within the last ~ 100 million to billion years on Mars [e.g., Dickson *et al.*, 2008;
437 Baker *et al.*, 2010; Hartmann *et al.*, 2014; Fassett *et al.*, 2014; Baker and Head, 2015; Berman
438 *et al.*, 2015]. Smaller-scale glacier-like forms have probably been active more recently, for ex-
439 ample small-scale lobate glaciers in Greg crater (38.5° S, 113° E) have been dated to have been
440 active 10-40 My ago [Hartmann *et al.*, 2014]. Such relatively small lobate debris-covered glaciers
441 are of a similar scale as the systems that formed the possible moraine deposits that are present
442 below gullies in some of the craters studied here, and their timing corresponds well with the
443 timing of the most recent glacial episode that we found in Talu crater. The end of this latest

444 glacial episode marks the start of the gully formation on crater walls formerly occupied by viscous-
445 flow features and glacial deposits, and is distinct from the much larger glacial events of >100
446 Ma. The presence of multiple glacial episodes on Mars, and their interaction with gullies, raises
447 the question how many glacial/post-glacial cycles have modified Amazonian landscapes on Mars.

448 **4.3 Paleoclimatic implications**

449 The morphological evidence for one or more cycles of gully activity and the good cor-
450 relation between the number and extent of these cycles and host crater age is in agreement with
451 previous findings that Mars has undergone numerous climatic changes, likely forced by orbital
452 variations [e.g., *Head et al.*, 2003; *Smith et al.*, 2016].

453 The association between LDM, glacial activity and gully-activity in many Martian craters
454 suggests that the abundance of water-ice has influenced the evolution of gullies in glaciated
455 landscapes on Mars. Water ice is the main component of the LDM and glacial deposits, and
456 the extent of former glaciers is generally strongly correlated with the distribution of gullies.
457 This suggests that gully formation may be linked to glacial activity, further suggesting that some
458 gullies may have formed by melting of ice within the LDM or glacial deposits. On the other
459 hand, the large gully-systems in the very young Istok, Gasa and Galap craters, which are free
460 of LDM and glacial deposits, show that extensive gully activity may also occur in the absence
461 of LDM and glacial deposits. These gullies may have formed by aqueous flows, dry CO₂-triggered
462 flows, or a combination as follows. Obliquity has hardly exceeded 35° since the formation of
463 Istok, Gasa and Galap craters, which may explain the absence of LDM and glacial features
464 in these craters. Nevertheless, obliquity may have been sufficiently high for snow accumula-
465 tion and melting in alcoves [e.g., *Head et al.*, 2008; *Williams et al.*, 2009], resulting in aque-
466 ous gully-activity [*De Haas et al.*, 2015a]. Such a mechanism is supported by the morphol-
467 ogy of the gully-fan deposits in Istok crater which closely resemble aqueous debris flows on
468 Earth [*Johnsson et al.*, 2014; *De Haas et al.*, 2015a]. Additionally, the sedimentology in ver-
469 tical walls along incised gully-channels and gully morphometry in Galap crater are consistent
470 with predominant formation by debris flows [*De Haas et al.*, 2015b]. Gasa crater formed in-
471 side a larger host crater, impacting into the remnants of debris-covered glaciers formed ear-
472 lier in the Amazonian. *Schon and Head* [2012] suggest that the Gasa impact penetrated into
473 the southern portion of this glacier, and that this ice provided a source of meltwater that formed
474 the gullies in Gasa crater. Slope stability analyses on the gully-alcoves in Gasa crater indeed
475 suggest that liquid H₂O was present in the formation of the gully-alcoves [*Okubo et al.*, 2011].

476 Moreover, morphometric analyses performed by *Conway and Balme* [2016] imply that the gul-
477 lies in these craters have been carved by liquid water. On the other hand, the regions where
478 H₂O is expected to accumulate are likely the same regions where CO₂ may be expected to
479 accumulate, and present-day gully activity related to CO₂ frost has been observed to modify
480 gullies in Gasa crater [*Dundas et al.*, 2010]. *Dundas et al.* [2010] observed movement of meter-
481 scale boulders and topographic changes in two separate channels and aprons, showing that sed-
482 iment transport in the gullies in Gasa crater is ongoing today. Additionally, recent smaller-scale
483 gully activity that may be related to CO₂ frost has amongst others been observed in Palikir
484 crater [*Dundas et al.*, 2012; *Vincendon*, 2015] and Corozal crater [*Dundas et al.*, 2010, 2015;
485 *Vincendon*, 2015]. These are both old craters (Corozal ~500 Ma; Palikir ~2.8 Ga) hosting ev-
486 idence for former glaciation, which shows that even if the distribution of gullies is strongly
487 correlated to former glacial deposits their formative mechanisms might not be uniquely related
488 to liquid water. However, multiple processes acting simultaneously, sequentially, or cyclically
489 within the same steep catchment or chute on Earth is normal [e.g., *Blair and McPherson*, 2009].
490 Hence, finding evidence for dry mass wasting within a steep gully chute is far from defini-
491 tive evidence of gully formation by dry processes only.

492 In short, these observations cannot determine whether aqueous or CO₂-triggered flows
493 contributed most substantially to gully formation. Yet, the intimate relation between LDM, glacial
494 deposits and gully deposits in older craters suggest the presence of periods wherein liquid wa-
495 ter plays an important role in gully formation. The observed relation between gullies and LDM
496 and glacial deposits shows that ice is abundant on many Martian midlatitude and polar crater
497 walls during glacial episodes, and that melting of this reservoir is consistent with the observed
498 stratigraphy. Further research would be needed to evaluate the potential of CO₂ to (partly) ex-
499 plain these stratigraphic relationships. The Martian climate has varied substantially over time,
500 and it is likely that the processes of gully formation and modification may have varied accord-
501 ingly.

502 **4.4 Potential spatial variations**

503 The present study is a first attempt to quantitatively study the temporal evolution of Mar-
504 tian gullies. Although we have used all publicly available HiRISE DTMs that host gullies and
505 for which host crater dating was possible, and even extended these with 8 of our own DTMs
506 this study is based on gullies in 19 craters only. Therefore, we can hardly take into account
507 any local and/or spatial effects on the temporal evolution of gullies. These are, however, prob-

ably important as there is a strong latitudinal control on the distribution and orientation of Martian gullies [e.g., *Balme et al.*, 2006; *Dickson et al.*, 2007; *Kneissl et al.*, 2010; *Harrison et al.*, 2015] and LDM and glacial deposits [e.g., *Squyres*, 1979; *Milliken et al.*, 2003; *Head et al.*, 2003; *Souness et al.*, 2012; *Brough et al.*, 2016]. Moreover, *Dickson et al.* [2015] show that there is a latitudinal control on the interaction between LDM deposition, removal and gully activity. They suggest that in the lower midlatitudes (30-40°) gullies go through cyclical degradation and removal, whereas gullies go through cycles of burial and exhumation of inverted gully channels in the transitional latitude band between dissected and preserved LDM (40-50°). The study by *Dickson et al.* [2015] focuses on LDM-hosted gullies, however, and does not consider gullies with alcoves that incise into bedrock, in contrast to this study.

To further explore the spatial imprint on the temporal evolution of Martian gullies, the quantitative temporal dataset presented here needs to be extended. A larger quantitative temporal dataset may ultimately enable separating spatial and temporal trends, which will further enhance our understanding of the spatio-temporal evolution of Martian gullies and may ultimately advance our understanding of their formation processes and the role of volatiles therein. Moreover, with a larger sample size, latitudinal variations in the present-day state of glaciation on Mars and their relation with gullies may potentially serve as analogues for temporal variations [i.e., the concept of space-for-time substitution; *Pickett*, 1989].

5 Conclusions

This paper quantitatively constrains and explains the temporal evolution of Martian gullies. To this end, the size of gullies, determined from HiRISE elevation models, and the relation between gullies, LDM deposits and glacial deposits are compared with host crater age in 19 craters on Mars.

Our results indicate that the size of gullies is unrelated to host crater age. Gully-size in very young host craters of a few million years old is similar to gully size in old host craters over a billion years old. Gullies on the walls of very young impact craters are free of LDM deposits (< a few Myr old), whereas they become increasingly influenced by LDM and glacial activity with increasing crater age. Gullies in craters of a few million to few tens of millions years old are typically affected by the LDM but not by glacial activity, while gullies in host craters of a few tens of millions years old or older are generally affected by both the LDM and glacial deposits.

539 These observations suggest that, after their formation in fresh craters, gullies may go through
540 repeated sequences of (1) LDM deposition and reactivation and (2) glacier formation and re-
541 moval, and the formation of new gully systems. Both sequences are likely governed by obliquity-
542 driven climate changes and may limit gully growth and remove or bury entire gully-fan de-
543 posits, thereby explaining the similar size of gullies in young and old host craters.

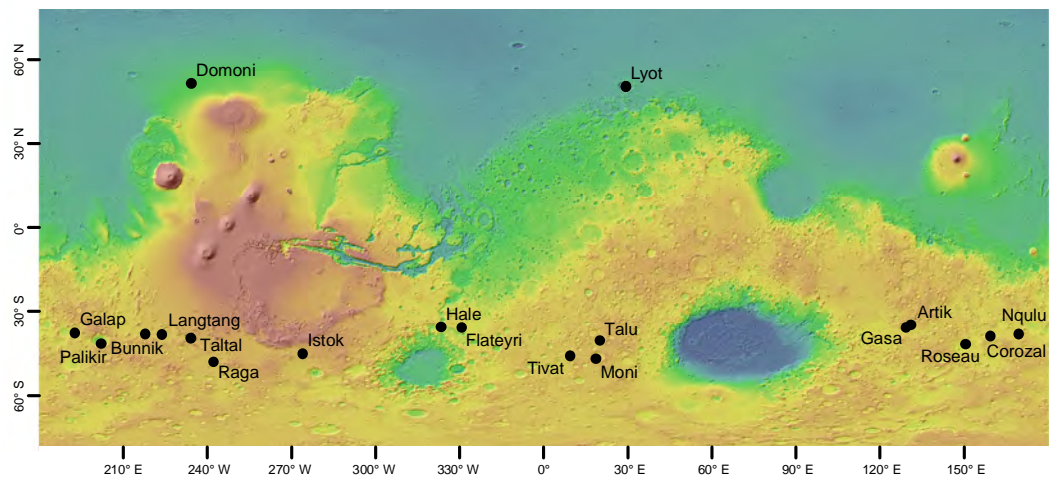
544 The temporal evolution of gullies can be summarized as follows. Following crater for-
545 mation gullies may rapidly form on the highly-fractured and oversteepened walls of the fresh
546 impact crater. Over time, the crater wall stabilizes and rates of geomorphic activity and gully
547 growth decrease. When obliquity is favorable, there is LDM deposition on top of the gullies,
548 which largely hampers further gully-alcove growth into bedrock mainly because geomorphic
549 flows now originate from the LDM deposits rather than the original crater-wall material. There
550 may be several sequences of LDM removal and deposition, until local conditions allow for suf-
551 ficient accumulation of snow/ice on the gullied crater-wall for the formation of glaciers. These
552 glaciers probably remove or bury the gully deposits, and leave behind a smoothed, oversteep-
553 ened, crater wall rich in loose material after their retreat. The crater wall conditions follow-
554 ing glacier retreat favor enhanced rates of geomorphic activity and enable rapid growth of new
555 gullies and if time permits the above described sequence of gully evolution may repeat itself.

556 The association between LDM, glaciers and gullies suggests a strong control of water
557 on the evolution of gullies. Meltwater of LDM and glaciers may have resulted in gully-formation
558 by aqueous flows, especially as the distribution of gullies often closely coincides with the ex-
559 tent of former glaciers. Yet, the role of liquid water remains debatable, as present-day gully
560 activity unrelated to liquid water is observed in some of the gullies formed after retreat of glaciers
561 and in the absence of LDM and glacial deposits in the youngest gullied craters in our dataset.
562 The Martian climate has varied substantially over time, and the dominant gully-forming mech-
563 anisms likely varied accordingly.

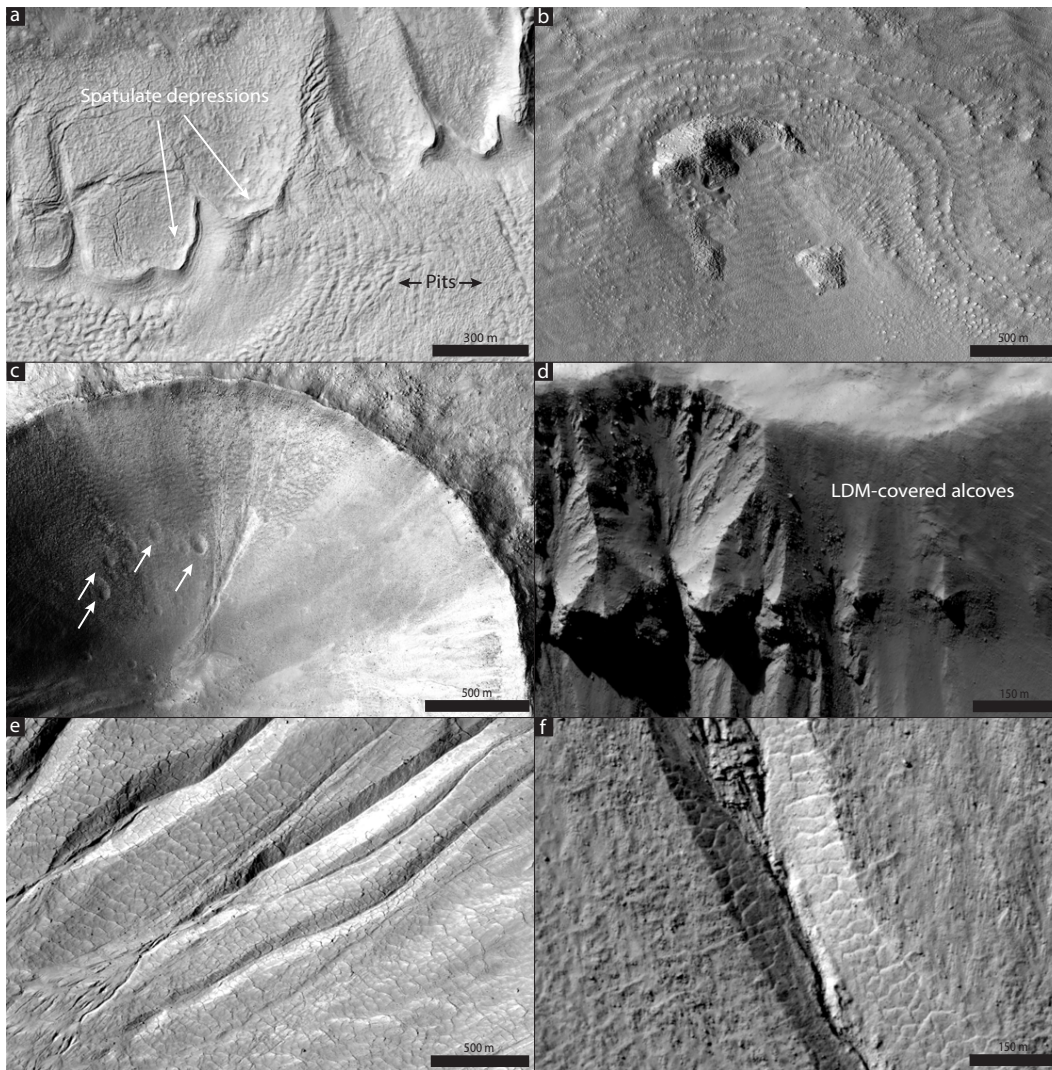
564 **Acknowledgments**

565 Reviewers will be thanked. TdH is funded by the Netherlands Organization for Scientific Re-
566 search (NWO) via Rubicon grant 019.153LW.002. SJC and MRB are funded by a Leverhulme
567 Trust grant RPG-397. MRB was supported also by the UK Space Agency (Grant ST/L00643X/1)
568 and the UK Science and Technology Facilities Council (grant ST/L000776/1). FEGB is funded
569 by STFC grant ST/N50421X/1. PMG is funded by the UK Space Agency (grant ST/L000254X/1),

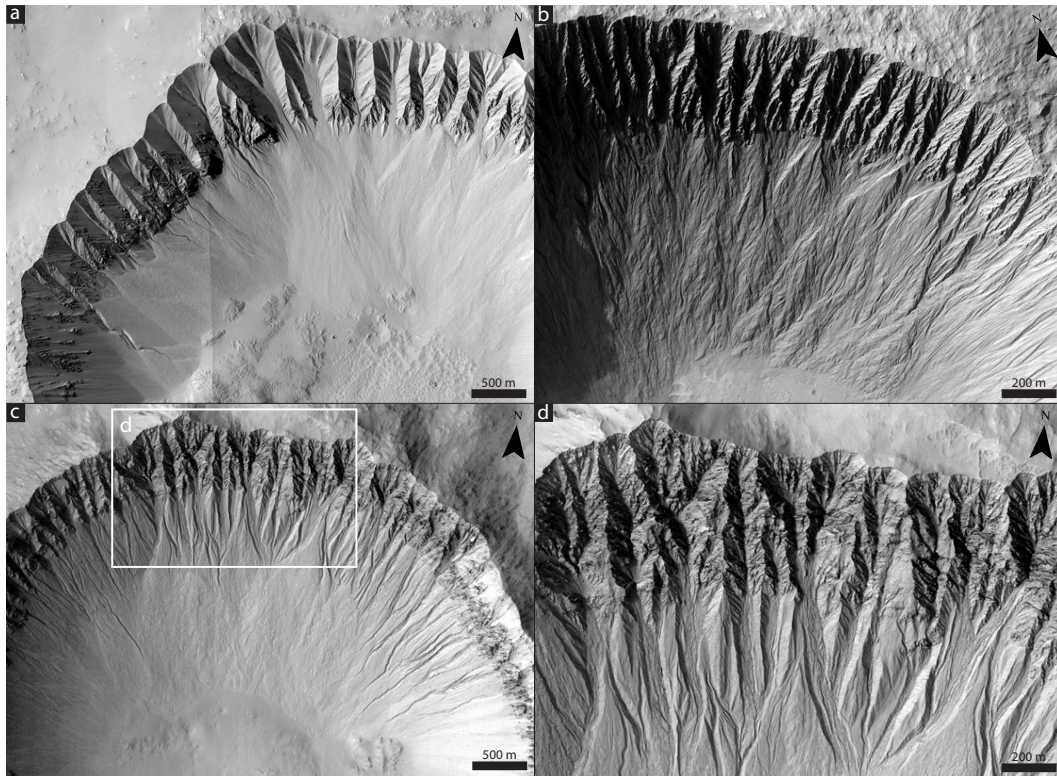
570 and acknowledges the UK NASA RPIF at University College London for DTM processing fa-
571 cilities.



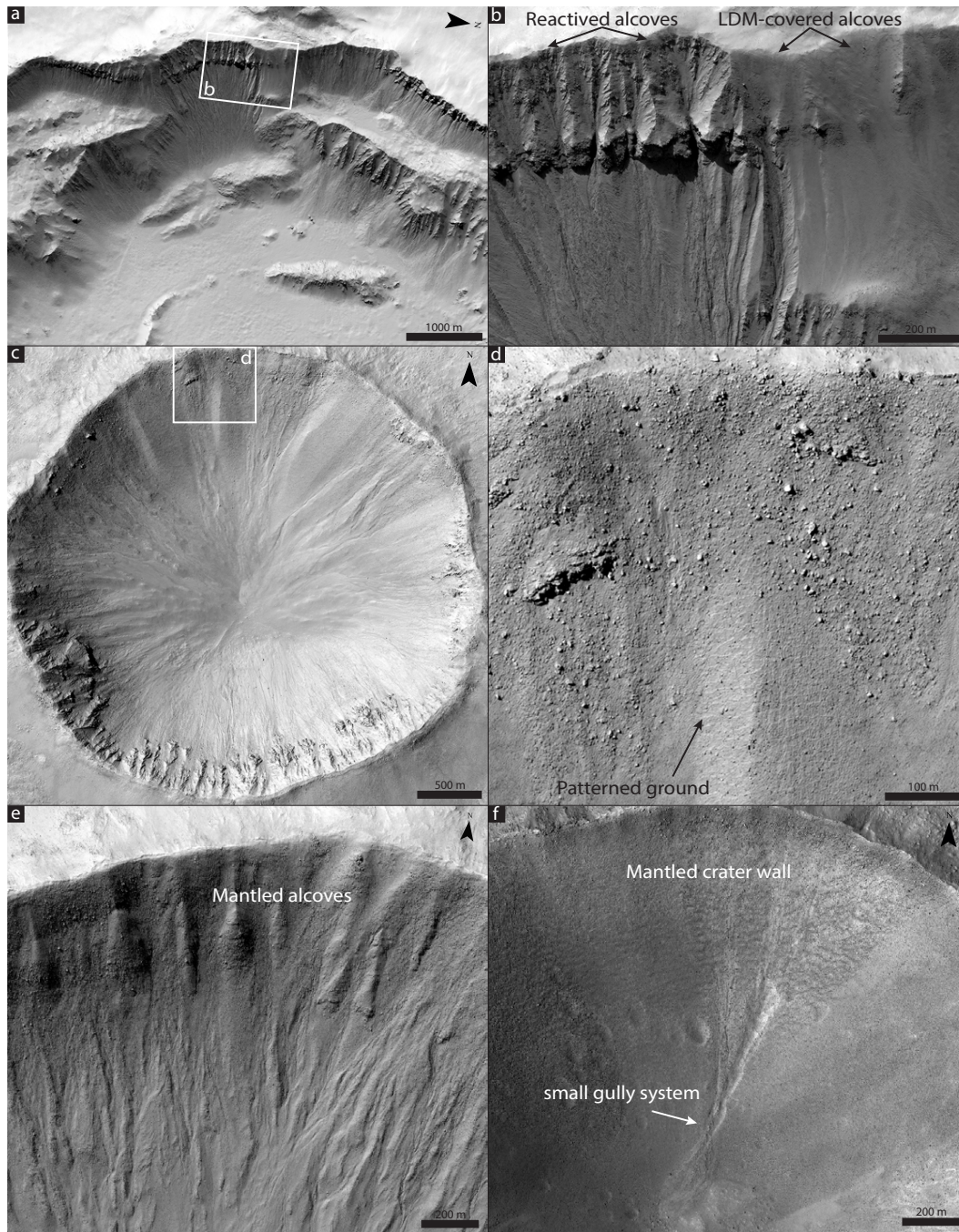
572 **Figure 1.** Study crater locations. Background, color-keyed and relief-shaded, topography is from the Mars
573 Orbiter Laser Altimeter (MOLA, red is high elevation, blue is low elevation).



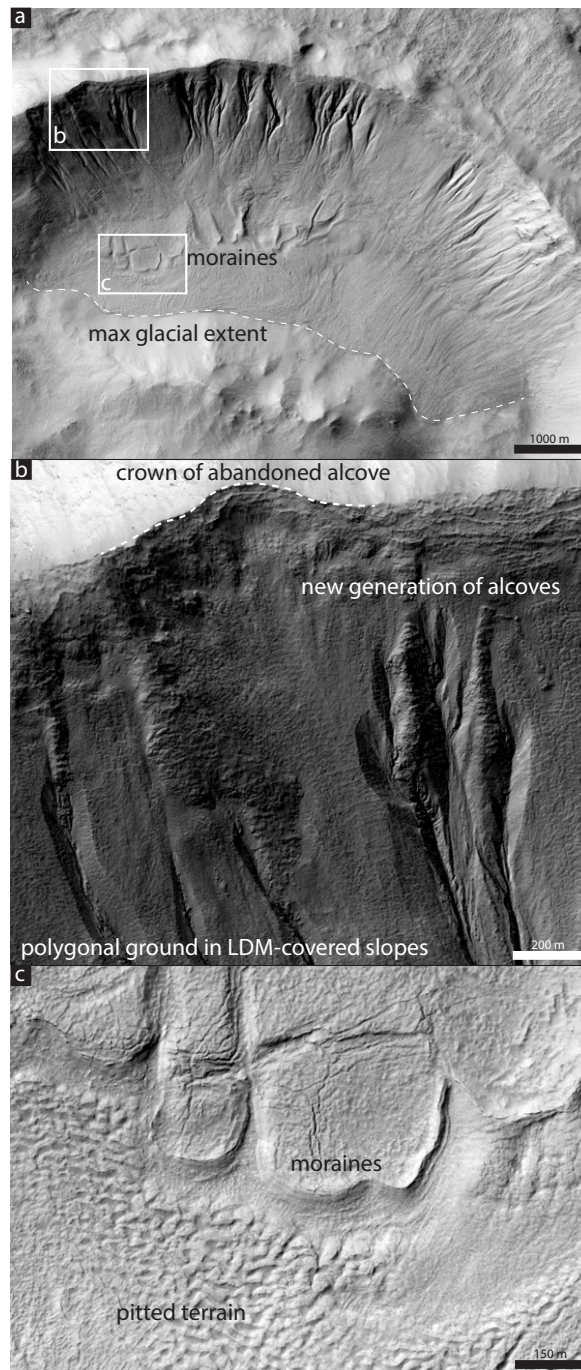
574 **Figure 2.** Examples of morphological evidence used to classify craters as influenced by the latitude-
 575 dependent mantle and/or influenced by past or present glaciation: (a) Arcuate spatulate depressions, which we
 576 interpret as moraine deposits, at the headward margin of an LDA on the floor of Langtang crater. Circular to
 577 elongate pits on the surface of the LDA support an ice-rich composition (HiRISE image ESP_023809_1415).
 578 (b) Horseshoe-shaped viscous flow around a topographic obstacle on the floor of Talu crater. Sub-parallel
 579 ridges near the margins of the flow are consistent with a compressional regime within flowing ice
 580 (HiRISE image ESP_011672_1395). (c) Softening of topography in the interior of Tivat crater by LDM
 581 materials that partially infill small impact craters (white arrows) on the interior crater wall (HiRISE image
 582 ESP_012991_1335). *Levy et al. [2009]* suggest that the gullies on this crater wall formed within the LDM
 583 deposits. (d) Infilling and softening of gully topography in Domoni crater by accumulations of LDM. The
 584 mantle obscures the fractured bedrock into which the unmantled gullies (on the left of the panel) are incised
 585 (HiRISE image ESP_016213_2315). (e) Pervasively polygonized LDM materials incised by gullies on the
 586 wall of Talu crater (HiRISE image ESP_011672_1395). (f) Polygonized walls of a gully alcove in Langtang
 587 crater, providing evidence for gully incision into an ice-rich mantle (HiRISE image ESP_023809_1415).



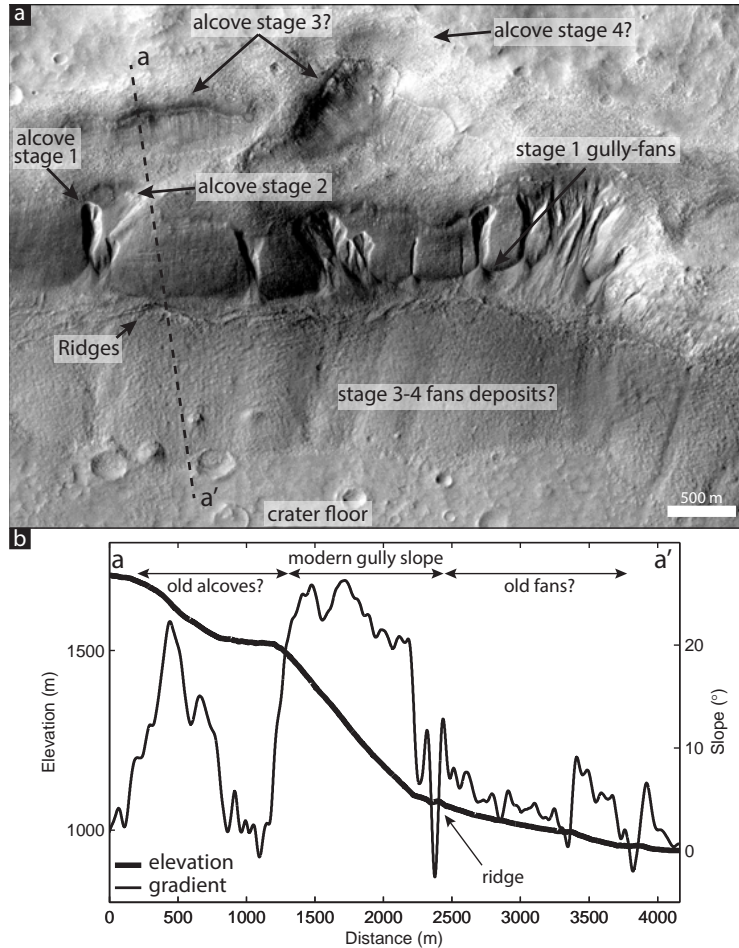
588 **Figure 3.** Morphology of young craters. The gully-alcoves have a crenulated shape and cut into the
589 upper crater rim, exposing fractured and highly brecciated bedrock containing many boulders. (a) Gasa
590 crater (HiRISE images ESP_014081_1440 and ESP_021584_1440). (b) Istok crater (HiRISE image
591 PSP_006837_1345). (c) Galap crater (HiRISE image ESP_012549_1420). (d) Detail of Galap crater alcoves.



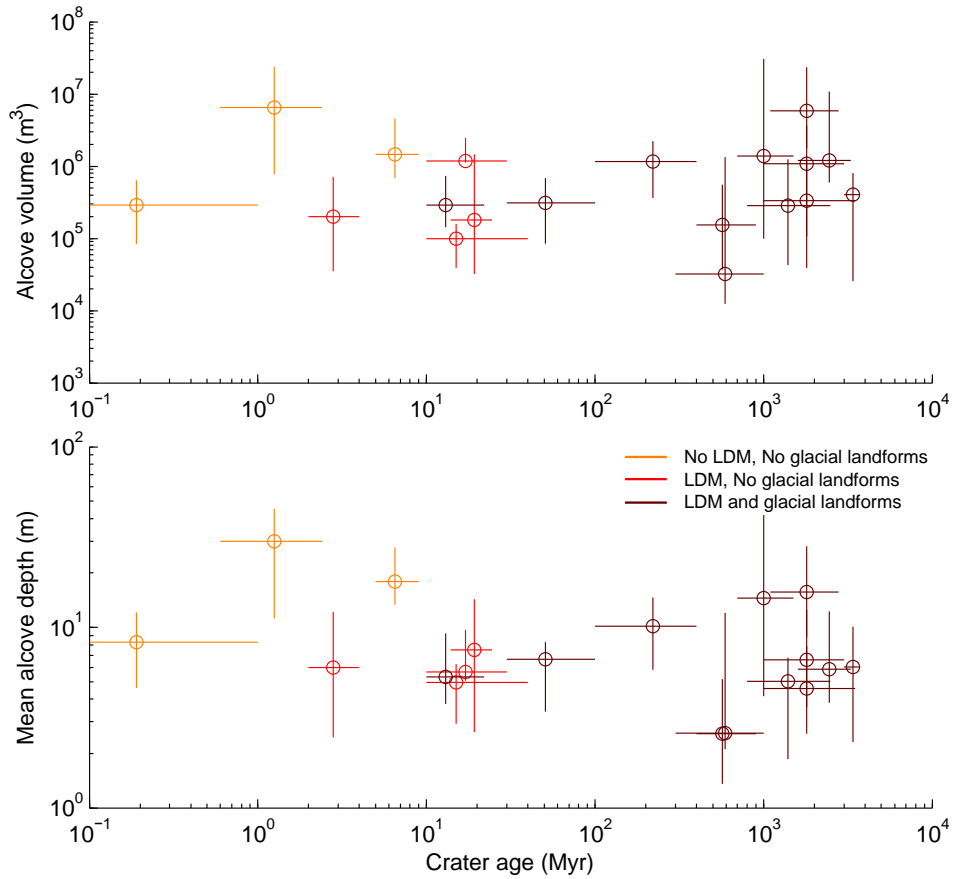
592 **Figure 4.** Interaction between gullies and LDM in Domoni, Raga, Roseau and Tivat craters. (a) West-
 593 ern wall of Domoni with abundant gullies. Evidence for former glaciation is absent (HiRISE image:
 594 ESP_016714_2315). (b) Detail of gully-alcoves: the gully-alcoves in the right side of the images are cov-
 595 ered by LDM deposits, whereas the gully-alcoves on the left side of the image have been reactivated since the
 596 last episode of LDM emplaced and therefore these alcoves are largely to completely free of LDM deposits.
 597 (c) Raga crater (HiRISE image: ESP_014011_1315). (d) Detail of gully-alcoves in Raga crater with soft-
 598 ened topography and patterned ground. (e) Detail of pole-facing gullies covered by LDM deposits in Roseau
 599 crater (HiRISE image: ESP_024115_1380). (f) Mantled pole-facing wall of Tivat crater (HiRISE image:
 600 ESP_012991_1335).



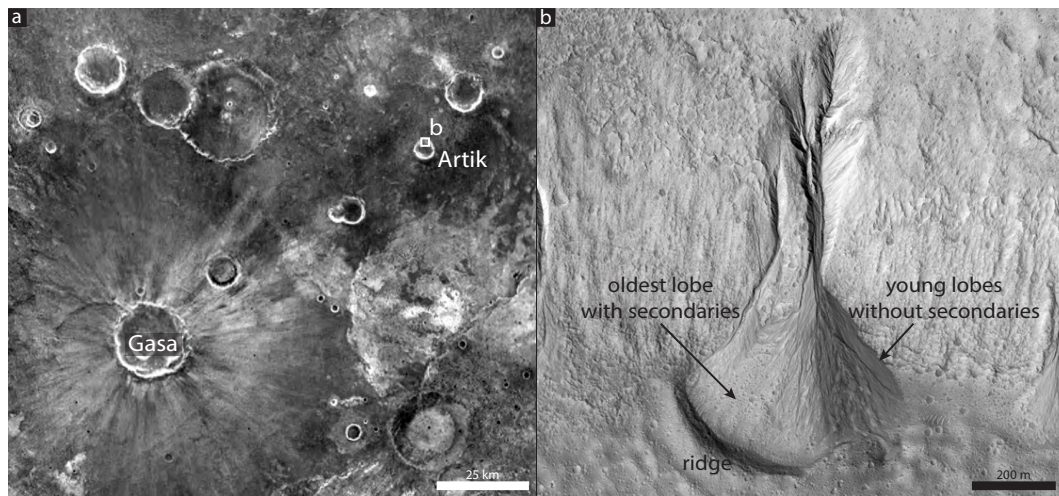
601 **Figure 5.** Multiple generations of alcoves and glacial advances in Langtang crater. (a) Glacial extent. CTX
 602 image F10_039752_1419_XI_38S142W. (b) Detail of the crater slope, showing the crown of a former, now
 603 abandoned, alcove and younger smaller generations of alcoves. The crater slope is covered by a thick layer
 604 of ice-rich material, as demonstrated by the shape of the youngest alcove incisions and polygonal patterned
 605 ground on top of the crater wall. The new alcove incises by more than 25 m into the crater wall. HiRISE
 606 image: ESP_023809_1415. (c) Detail of the moraine deposits and the pitted terrain, which originates from
 607 sublimation till. HiRISE image: ESP_023809_1415.



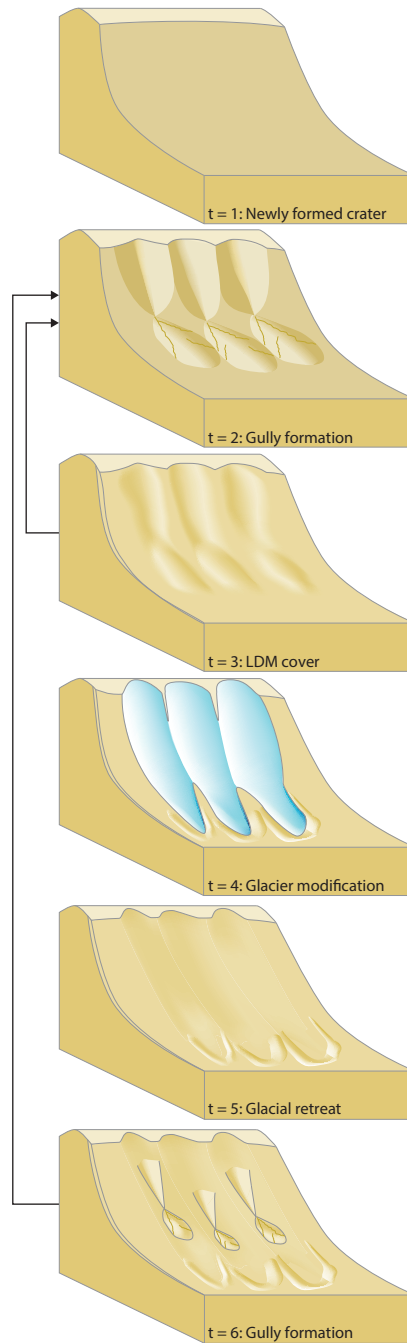
608 **Figure 6.** Multiple alcove and fan generations in Bunnik crater. (a) At least two generations of alcoves
 609 (stage 1 and 2), and potentially four generations of alcoves (stage 3 and 4), can be recognized on the crater
 610 wall. Below the youngest gullies (stage 1) arcuate ridges can be identified, under which the remnants of the
 611 lower parts of extensive fans can be recognized (note the difference in amount of superposed craters on these
 612 fan deposits and the crater floor). CTX image F10_039752_1419_XI_38S142W. (b) Elevation and gradient
 613 along line a-a'.



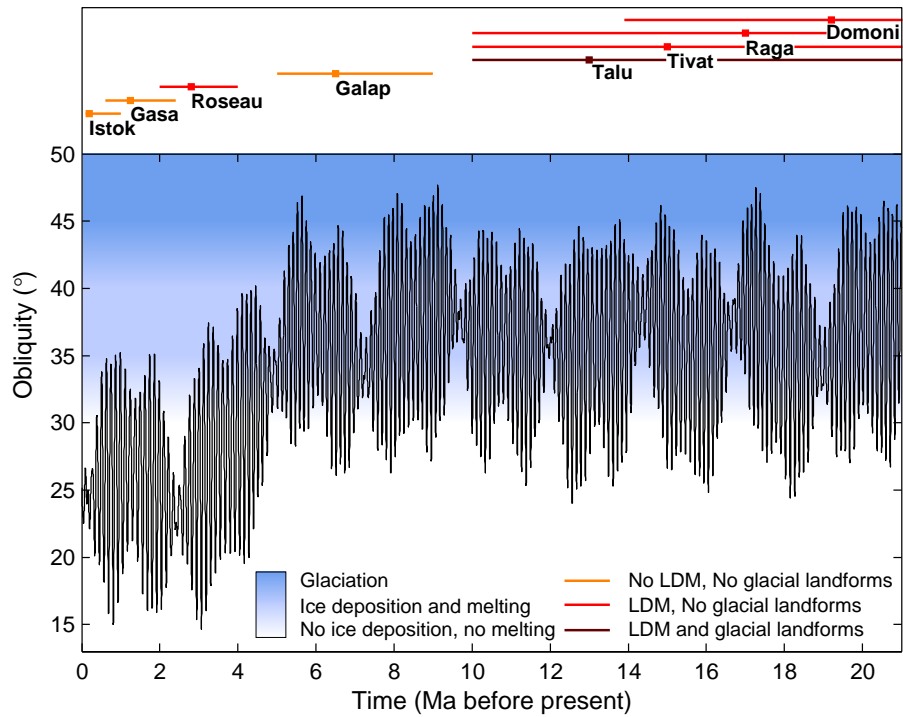
614 **Figure 7.** Gully-alcove size as a function of crater age. (a) Crater age versus alcove volume. (b) Crater
 615 age versus mean alcove depth. The circles are the best fit crater ages and the median backweathering rates
 616 per crater. Bars denote minimum and maximum crater age and the 10th and 90th percentile alcove size of the
 617 measured gully-alcoves within each crater.



618 **Figure 8.** Artik crater (~ 590 Ma). (a) Themis nighttime infrared image showing the distribution of the
619 Gasa impact rays from which the large population of secondaries in Artik crater originate. (b) Gully in Artik
620 crater. The oldest lobe of the crater is covered by secondaries and thus older than 1.25 Ma, whereas the su-
621 perposed gully-fan lobes are free of secondaries and are thus younger than 1.25 Ma [cf. *Schon et al.*, 2009;
622 *De Haas et al.*, 2013] (HiRISE image: ESP_012314_1450).



623 **Figure 9.** Conceptual model of the temporal evolution of gullies on Mars. (t=1) The highly-fractured and
 624 unstable walls of newly formed impact craters are prone to gully formation. (t=2) As a result, large gullies
 625 may rapidly form. Such gullies may typically cut into the crater rim. (t=3) During high-obliquity periods
 626 the gullies may be covered by LDM deposits, which impedes further gully-alcove growth. Subsequently,
 627 gullies may reactivate and transport the LDM deposits in the gully alcoves to the gully-fan until a new mantling
 628 episode commences. Gullies may experience multiple repeats of these cycles. (t=4) During favorable obliquity
 629 periods glaciers may form on the crater wall removing or burying the gully deposits, and forming a
 630 moraine deposit at the toe of glacier. (t=5) Following glacial retreat a smoothed crater wall and moraine
 631 deposits remain. (t=6) New gullies may now form within the formerly glaciated crater wall. Such gullies
 632 typically have v-shaped and elongated alcoves and do not extend to the top of the crater wall. The gullies may
 633 enlarge until there is another episode of LDM emplacement or glaciation.



634 **Figure 10.** Martian obliquity in the last 21 My [*Laskar et al.*, 2004], obliquity thresholds for melting [*Head*
 635 *et al.*, 2003] and glaciation [*Baker et al.*, 2010], and study crater ages and ice-related morphology within these
 636 craters. Young craters (Istok, Gasa and Galap) have no evidence for LDM and glacial landforms and may
 637 have formed by melting of restricted amounts of snow/ice or CO₂ triggered flows. Older craters that have
 638 experienced substantial high-obliquity periods (>40-45°) are affected by LDM and/or glacial activity and
 639 may have undergone multiple gully accumulation-degradation cycles.

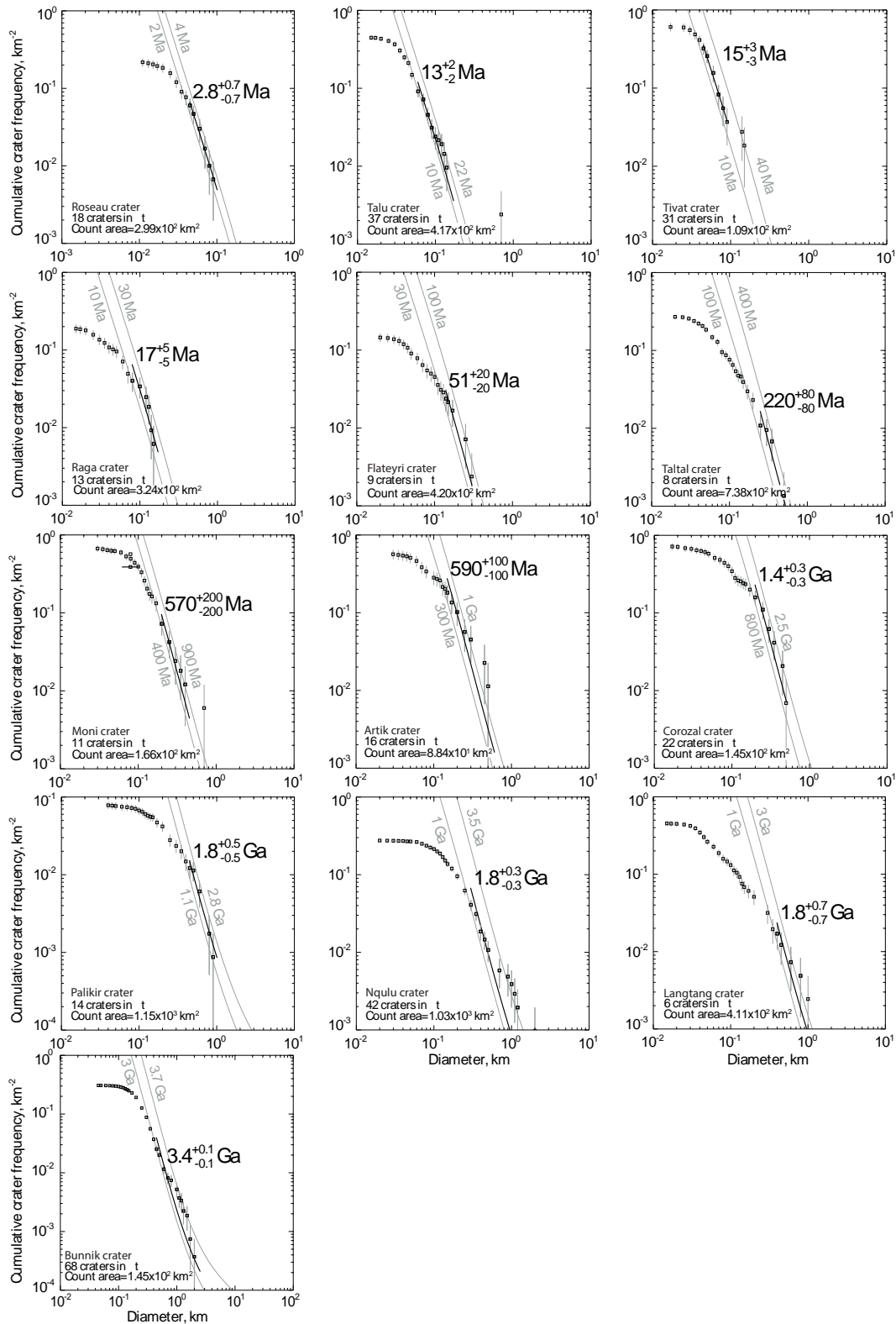
Table 1. Study crater characteristics.

Crater	Latitude	Longitude	Diameter (km)	Landform assemblage	Age	Age source
Istok	45.1°S	274.2°E	4.7	No LDM, No glacial landforms	0.19 (0.1–1.0) Ma	<i>Johnsson et al.</i> [2014]
Gasa	35.7°S	129.5°E	6.5	No LDM, No glacial landforms	1.25 (0.6–2.4) Ma	<i>Schon et al.</i> [2009]
Roseau	41.7°S	150.6°E	6.2	LDM, No glacial landforms	2.8 (2–4) Ma	Figure A.1
Galap	37.7°S	192.9°E	5.6	No LDM, No glacial landforms	6.5 (5–9) Ma	<i>De Haas et al.</i> [2015c]
Talu	40.3°S	20.1°E	9.1	LDM & glacial landforms	13 (10–22) Ma	Figure A.1
Tivat	45.9°S	9.5°E	3.1	LDM, No glacial landforms	15 (10–40) Ma	Figure A.1
Raga	48.1°S	242.4°E	3.4	LDM, No glacial landforms	17 (10–30) Ma	Figure A.1
Domoni	51.4°N	234.2°E	14	LDM, No glacial landforms	19.2 (13.9–24.5) Ma	<i>Viola et al.</i> [2015]
Flateyri	35.9°S	330.9°E	9.5	LDM & glacial landforms	51 (30–100) Ma	Figure A.1
Taltal	39.5°S	234.4°E	9.8	LDM & glacial landforms	220 (100–400) Ma	Figure A.1
Moni	47.0°S	18.8°E	5.0	LDM & glacial landforms	570 (400–900) Ma	Figure A.1
Artik	34.8°S	131.0°E	5.2	LDM & glacial landforms	590 (300–1000) Ma	Figure A.1
Hale	35.5°S	323.5°E	140	LDM & glacial landforms	~ 1 Ga	<i>Jones et al.</i> [2011]
Corozal	38.7°S	159.4°E	8.0	LDM & glacial landforms	1.4 (0.8–2.5) Ga	Figure A.1
Palikir	41.5°S	202.2°E	16	LDM & glacial landforms	1.8 (1.1–2.8) Ga	Figure A.1
Nqulu	37.9°S	169.6°E	20	LDM & glacial landforms	1.8 (1–3.5) Ga	Figure A.1
Langtang	38.1°S	224.0°E	9.2	LDM & glacial landforms	1.8 (1–3) Ga	Figure A.1
Lyot	50.5°N	29.4°E	115	LDM & glacial landforms	n.a. (1.6–3.3) Ga	<i>Dickson et al.</i> [2009]
Bunnik	37.8°S	217.9°E	28	LDM & glacial landforms	3.4 (3–3.7) Ga	Figure A.1

641 **Table 2.** List of data sources and vertical accuracy for the DTMs used to calculate alcove volumes. DTMs
 642 from the University of Arizona were downloaded from the HiRISE website (<http://www.uahirise.org/dtm/>),
 643 the other DTMs were made by the authors. DTM's with credit Open University or Birckbeck University of
 644 London were made with SocetSet, DTM's with credit University of Texas were made with the Ames Stereo
 645 Pipeline. Vertical precision was estimated via the method of *Kirk et al.* [2008].

Crater	HiRISE image 1	Pixel scale image 1 (m)	HiRISE image 2	Pixel scale image 2 (m)	Convergence angle ($^{\circ}$)	Vertical precision (m)	DTM credit
Istok	PSP.006837.1345	0.250	PSP.007127.1345	0.258	20.1	0.14	Open University
Gasa (1)	ESP.021584.1440	0.255	ESP.022217.1440	0.279	20.8	0.15	University of Arizona
Gasa (2)	ESP.014081.1440	0.507	ESP.014147.1440	0.538	20.7	0.28	University of Arizona
Roseau	ESP.024115.1380	0.252	ESP.011509.1380	0.255	7.2	0.40	University of Texas
Galap	PSP.003939.1420	0.256	PSP.003939.1420	0.291	21.7	0.15	Open University
Talu	ESP.011672.1395	0.26	ESP.011817.1395	0.26	15.7	0.18	Open University
Tivat	ESP.012991.1335	0.25	ESP.013624.1335	0.26	17.3	0.17	University of Arizona
Raga	ESP.014011.1315	0.25	ESP.014288.1315	0.27	21.1	0.14	University of Arizona
Domoni (1)	ESP.016213.2315	0.30	ESP.016714.2315	0.31	18.1	0.19	University of Arizona
Domoni (2)	ESP.016846.2320	0.32	ESP.016569.2320	0.30	15.7	0.22	University of Arizona
Flateyri	ESP.022315.1440	0.257	ESP.030517.1440	0.258	0.8	3.7	University of Texas
Taltal	ESP.037074.1400	0.505	ESP.031259.1400	0.502	5.9	0.98	University of Texas
Moni	PSP.007110.1325	0.26	PSP.006820.1325	0.25	19.2	0.15	University of Arizona
Artik	ESP.012459.1450	0.27	ESP.012314.1450	0.25	14.5	0.21	University of Arizona
Hale (1)	ESP.012241.1440	0.26	ESP.012663.1440	0.26	15.3	0.19	University of Arizona
Hale (2)	ESP.030715.1440	0.29	ESP.030570.1440	0.26	15.7	0.20	University of Arizona
Hale (3)	PSP.002932.1445	0.26	PSP.003209.1445	0.27	24.9	0.12	Birkbeck University of London
Corozal	PSP.006261.1410	0.25	ESP.014093.1410	0.29	28.7	0.10	University of Arizona
Palikir	PSP.005943.1380	0.25	ESP.011428.1380	0.26	16.9	0.17	University of Arizona
Nqulu	PSP.004085.1420	0.27	PSP.004019.1420	0.25	20.4	0.14	Birkbeck University of London
Langtang	ESP.024099.1415	0.28	ESP.023809.1415	0.25	30.9	0.09	University of Arizona
Lytot	PSP.008823.2310	0.31	PSP.009245.2310	0.32	17.2	0.20	University of Arizona
Bunnik	PSP.002659.1420	0.26	PSP.002514.1420	0.25	13.6	0.21	University of Arizona

A: Host crater dating



647 **Figure A.1.** Crater-size-frequency distributions of dated craters. Crater ages were de-
 648 fined based on the crater-size-frequency distribution using the chronology model of *Hart-*
 649 *mann and Neukum* [2001] and the production function of *Ivanov* [2001]. Roseau crater:
 650 count performed on CTX image B05_011443_1380_XI_42S209W. Talu crater: count per-
 651 formed on CTX image B05_011672_1394_XN_40S339W. Tivat crater: count performed on
 652 CTX image B10_013624_1338_XN_46S350W. Raga crater: count performed on CTX im-
 653 age D10_031206_1316_XN_48S117W. Flateyri crater: count performed on CTX images
 654 P02_001745_1439_XN_36S029W and P15_007059_1438_XN_36S029W. Taltal crater: count per-

666 **References**

- 667 Arfstrom, J., and W. K. Hartmann (2005), Martian flow features, moraine-like ridges, and
 668 gullies: Terrestrial analogs and interrelationships, *Icarus*, 174(2), 321–335.
- 669 Aston, A., S. Conway, and M. Balme (2011), Identifying Martian gully evolution, *Geolog-*
 670 *ical Society, London, Special Publications*, 356(1), 151–169.
- 671 Baker, D. M., and J. W. Head (2015), Extensive Middle Amazonian mantling of debris
 672 aprons and plains in Deuteronilus Mensae, Mars: Implications for the record of mid-
 673 latitude glaciation, *Icarus*, 260, 269–288.
- 674 Baker, D. M., J. W. Head, and D. R. Marchant (2010), Flow patterns of lobate debris
 675 aprons and lineated valley fill north of Ismeniae Fossae, Mars: Evidence for extensive
 676 mid-latitude glaciation in the Late Amazonian, *Icarus*, 207(1), 186–209.
- 677 Ballantyne, C. K. (2002), Paraglacial geomorphology, *Quaternary Science Reviews*, 21(18),
 678 1935–2017.
- 679 Balme, M., N. Mangold, D. Baratoux, F. Costard, M. Gosselin, P. Masson, P. Pinet,
 680 and G. Neukum (2006), Orientation and distribution of recent gullies in the southern
 681 hemisphere of Mars: observations from High Resolution Stereo Camera/Mars Express
 682 (HRSC/MEX) and Mars Orbiter Camera/Mars Global Surveyor (MOC/MGS) data,
 683 *Journal of Geophysical Research: Planets (1991–2012)*, 111(E5), E05,001.
- 684 Berman, D. C., W. K. Hartmann, D. A. Crown, and V. R. Baker (2005), The role of arcu-
 685 ate ridges and gullies in the degradation of craters in the Newton Basin region of Mars,
 686 *Icarus*, 178(2), 465–486.
- 687 Berman, D. C., D. A. Crown, and L. F. Bleamaster (2009), Degradation of mid-latitude
 688 craters on Mars, *Icarus*, 200(1), 77–95.
- 689 Berman, D. C., D. A. Crown, and E. C. Joseph (2015), Formation and mantling ages of
 690 lobate debris aprons on Mars: Insights from categorized crater counts, *Planetary and*
 691 *Space Science*, 111, 83–99.
- 692 Beyer, R., O. Alexandrov, and Z. Moratto (2014), Aligning terrain model and laser al-
 693 timeter point clouds with the Ames Stereo Pipeline, in *Lunar and Planetary Science*
 694 *Conference*, vol. 45, p. 2902.
- 695 Blair, T. C., and J. G. McPherson (2009), Processes and forms of alluvial fans, in *Ge-*
 696 *omorphology of Desert Environments*, edited by A. Parsons and A. Abrahams, pp.
 697 413–467, Springer Netherlands.

- 698 Brough, S., B. Hubbard, and A. Hubbard (2016), Former extent of glacier-like forms on
699 Mars, *Icarus*, 274, 37–49.
- 700 Broxton, M. J., and L. J. Edwards (2008), The Ames Stereo Pipeline: Automated 3D sur-
701 face reconstruction from orbital imagery, in *Lunar and Planetary Science Conference*,
702 vol. 39, p. 2419.
- 703 Cedillo-Flores, Y., A. H. Treiman, J. Lasue, and S. M. Clifford (2011), CO₂ gas fluidiza-
704 tion in the initiation and formation of Martian polar gullies, *Geophysical Research*
705 *Letters*, 38(21), L21,202.
- 706 Christensen, P. R. (2003), Formation of recent Martian gullies through melting of exten-
707 sive water-rich snow deposits, *Nature*, 422(6927), 45–48.
- 708 Christiansen, H. H. (1998), Nivation forms and processes in unconsolidated sediments, NE
709 Greenland, *Earth Surface Processes and Landforms*, 23(8), 751–760.
- 710 Church, M., and J. M. Ryder (1972), Paraglacial sedimentation: a consideration of fluvial
711 processes conditioned by glaciation, *Geological Society of America Bulletin*, 83(10),
712 3059–3072.
- 713 Conway, S. (This Issue), Gullies review, *Gullies special issue: Geological Society of Lon-*
714 *don*.
- 715 Conway, S. J. (2010), Debris flows on earth and mars, Ph.D. thesis, Open University.
- 716 Conway, S. J., and M. Balme (2016), A novel topographic parameterization scheme in-
717 dicates that martian gullies display the signature of liquid water, *Earth and Planetary*
718 *Science Letters*, 454, 36–45.
- 719 Conway, S. J., and M. R. Balme (2014), Decameter thick remnant glacial ice deposits on
720 Mars, *Geophysical Research Letters*, 41(15), 5402–5409.
- 721 Conway, S. J., M. R. Balme, J. B. Murray, M. C. Towner, C. H. Okubo, and P. M.
722 Grindrod (2011), The indication of Martian gully formation processes by slope–area
723 analysis, *Geological Society, London, Special Publications*, 356(1), 171–201.
- 724 Conway, S. J., M. R. Balme, M. A. Kreslavsky, J. B. Murray, and M. C. Towner (2015),
725 The comparison of topographic long profiles of gullies on Earth to gullies on Mars: a
726 signal of water on Mars, *Icarus*, 253, 189–204.
- 727 Costard, F., F. Forget, N. Mangold, and J. P. Peulvast (2002), Formation of Recent Mar-
728 tian Debris Flows by Melting of Near-Surface Ground Ice at High Obliquity, *Science*,
729 295(5552), 110–113.

- 730 De Haas, T., E. Hauber, and M. G. Kleinhans (2013), Local late Amazonian boulder
731 breakdown and denudation rate on Mars, *Geophysical Research Letters*, *40*, 3527–3531.
- 732 De Haas, T., E. Hauber, S. J. Conway, H. van Steijn, A. Johnsson, and M. G. Kleinhans
733 (2015a), Earth-like aqueous debris-flow activity on Mars at high orbital obliquity in the
734 last million years, *Nature Communications*, *6*:7543.
- 735 De Haas, T., D. Ventra, E. Hauber, S. J. Conway, and M. G. Kleinhans (2015b), Sedimen-
736 tological analyses of Martian gullies: the subsurface as the key to the surface, *Icarus*,
737 *258*, 92–108.
- 738 De Haas, T., S. J. Conway, and M. Krautblatter (2015c), Recent (Late Amazonian) en-
739 hanced backweathering rates on Mars: Paracratering evidence from gully alcoves,
740 *Journal of Geophysical Research: Planets*, *120*(12), 2169–2189.
- 741 Dickson, J., C. Fassett, and J. Head (2009), Amazonian-aged fluvial valley systems in
742 a climatic microenvironment on Mars: Melting of ice deposits on the interior of Lyot
743 Crater, *Geophysical Research Letters*, *36*, L08,201.
- 744 Dickson, J. L., and J. W. Head (2009), The formation and evolution of youthful gullies
745 on Mars: Gullies as the late-stage phase of Mars most recent ice age, *Icarus*, *204*(1),
746 63–86.
- 747 Dickson, J. L., J. W. Head, and M. Kreslavsky (2007), Martian gullies in the southern
748 mid-latitudes of Mars: Evidence for climate-controlled formation of young fluvial fea-
749 tures based upon local and global topography, *Icarus*, *188*(2), 315 – 323.
- 750 Dickson, J. L., J. W. Head, and D. R. Marchant (2008), Late Amazonian glaciation at
751 the dichotomy boundary on Mars: Evidence for glacial thickness maxima and multiple
752 glacial phases, *Geology*, *36*(5), 411–414.
- 753 Dickson, J. L., J. W. Head, T. A. Goudge, and L. Barbieri (2015), Recent climate cycles
754 on Mars: Stratigraphic relationships between multiple generations of gullies and the
755 latitude dependent mantle, *Icarus*, *252*, 83–94.
- 756 Dundas, C. M., A. S. McEwen, S. Diniega, S. Byrne, and S. Martinez-Alonso (2010),
757 New and recent gully activity on Mars as seen by HiRISE, *Geophysical Research Let-
758 ters*, *37*(7), L07,202.
- 759 Dundas, C. M., S. Diniega, C. J. Hansen, S. Byrne, and A. S. McEwen (2012), Seasonal
760 activity and morphological changes in Martian gullies, *Icarus*, *220*(1), 124–143.
- 761 Dundas, C. M., S. Diniega, and A. S. McEwen (2015), Long-Term Monitoring of Martian
762 Gully Formation and Evolution with MRO/HiRISE, *Icarus*, *251*, 244–263.

- 763 Fassett, C. I., J. S. Levy, J. L. Dickson, and J. W. Head (2014), An extended period of
764 episodic northern mid-latitude glaciation on Mars during the Middle to Late Amazo-
765 nian: Implications for long-term obliquity history, *Geology*, 42(9), 763–766.
- 766 Forget, F., R. M. Haberle, F. Montmessin, B. Levrard, and J. W. Head (2006), Formation
767 of glaciers on Mars by atmospheric precipitation at high obliquity, *Science*, 311(5759),
768 368–371.
- 769 Harrison, T. N., G. R. Osinski, L. L. Tornabene, and E. Jones (2015), Global documenta-
770 tion of gullies with the Mars Reconnaissance Orbiter Context Camera and implications
771 for their formation, *Icarus*, 252, 236–254.
- 772 Hartmann, W. K., and G. Neukum (2001), Cratering chronology and the evolution of
773 Mars, in *Chronology and evolution of Mars*, pp. 165–194, Springer.
- 774 Hartmann, W. K., V. Ansan, D. C. Berman, N. Mangold, and F. Forget (2014), Compre-
775 hensive analysis of glaciated martian crater Greg, *Icarus*, 228, 96–120.
- 776 Head, J. W., J. F. Mustard, M. A. Kreslavsky, R. E. Milliken, and D. R. Marchant (2003),
777 Recent ice ages on Mars, *Nature*, 426, 797–802.
- 778 Head, J. W., D. R. Marchant, and M. A. Kreslavsky (2008), Formation of gullies on Mars:
779 Link to recent climate history and insolation microenvironments implicate surface water
780 flow origin, *Proceedings of the National Academy of Sciences*, 105(36), 13,258–13,263.
- 781 Head, J. W., D. R. Marchant, J. L. Dickson, A. M. Kress, and D. M. Baker (2010), North-
782 ern mid-latitude glaciation in the Late Amazonian period of Mars: Criteria for the
783 recognition of debris-covered glacier and valley glacier landsystem deposits, *Earth and*
784 *Planetary Science Letters*, 294(3), 306–320.
- 785 Heldmann, J. L., and M. T. Mellon (2004), Observations of Martian gullies and con-
786 straints on potential formation mechanisms, *Icarus*, 168(2), 285 – 304.
- 787 Heldmann, J. L., O. B. Toon, W. H. Pollard, M. T. Mellon, J. Pitlick, C. P. McKay, and
788 D. T. Andersen (2005), Formation of Martian gullies by the action of liquid water
789 flowing under current Martian environmental conditions, *J. Geophys. Res.*, 110(E5),
790 E05,004.
- 791 Hubbard, B., R. E. Milliken, J. S. Kargel, A. Limaye, and C. Souness (2011), Geomor-
792 phological characterisation and interpretation of a mid-latitude glacier-like form: Hellas
793 Planitia, Mars, *Icarus*, 211(1), 330–346.
- 794 Ivanov, B. A. (2001), Mars/Moon cratering rate ratio estimates, in *Chronology and evolu-*
795 *tion of Mars*, pp. 87–104, Springer.

- 796 Johnsson, A., D. Reiss, E. Hauber, H. Hiesinger, and M. Zanetti (2014), Evidence for very
797 recent melt-water and debris flow activity in gullies in a young mid-latitude crater on
798 Mars, *Icarus*, 235, 37–54.
- 799 Jones, A., A. McEwen, L. Tornabene, V. Baker, H. Melosh, and D. Berman (2011), A ge-
800 omorphic analysis of Hale crater, Mars: The effects of impact into ice-rich crust, *Icarus*,
801 211(1), 259–272.
- 802 Kirk, R., E. Howington-Kraus, M. Rosiek, J. Anderson, B. Archinal, K. Becker, D. Cook,
803 D. Galuszka, P. Geissler, T. Hare, et al. (2008), Ultrahigh resolution topographic
804 mapping of Mars with MRO HiRISE stereo images: Meter-scale slopes of candidate
805 Phoenix landing sites, *Journal of Geophysical Research: Planets (1991–2012)*, 113(E3),
806 E00A24.
- 807 Kneissl, T., D. Reiss, S. Van Gasselt, and G. Neukum (2010), Distribution and orientation
808 of northern-hemisphere gullies on Mars from the evaluation of HRSC and MOC-NA
809 data, *Earth and Planetary Science Letters*, 294(3), 357–367.
- 810 Kneissl, T., S. van Gasselt, and G. Neukum (2011), Map-projection-independent crater
811 size-frequency determination in GIS environments - New software tool for ArcGIS,
812 *Planetary and Space Science*, 59(11), 1243–1254.
- 813 Kreslavsky, M., and J. Head (2002), Mars: Nature and evolution of young latitude-
814 dependent water-ice-rich mantle, *Geophysical Research Letters*, 29(15), doi:
815 10.1029/2002GL015392.
- 816 Kreslavsky, M. A., J. W. Head, and D. R. Marchant (2008), Periods of active permafrost
817 layer formation during the geological history of Mars: Implications for circum-polar
818 and mid-latitude surface processes, *Planetary and Space Science*, 56(2), 289–302.
- 819 Kumar, P. S., J. W. Head, and D. A. Kring (2010), Erosional modification and gully for-
820 mation at Meteor Crater, Arizona: Insights into crater degradation processes on Mars,
821 *Icarus*, 208(2), 608–620.
- 822 Laskar, J., A. Correia, M. Gastineau, F. Joutel, B. Levrard, and P. Robutel (2004), Long
823 term evolution and chaotic diffusion of the insolation quantities of mars, *Icarus*, 170(2),
824 343 – 364.
- 825 Levrard, B., F. Forget, F. Montmessin, and J. Laskar (2007), Recent formation and evo-
826 lution of northern Martian polar layered deposits as inferred from a Global Climate
827 Model, *Journal of Geophysical Research: Planets*, 112(E6), E06,012.

- 828 Levy, J., J. Head, D. Marchant, J. Dickson, and G. Morgan (2009), Geologically recent
829 gully–polygon relationships on Mars: Insights from the Antarctic Dry Valleys on the
830 roles of permafrost, microclimates, and water sources for surface flow, *Icarus*, 201(1),
831 113–126.
- 832 Levy, J., J. Head, J. Dickson, C. Fassett, G. Morgan, and S. Schon (2010a), Identification
833 of gully debris flow deposits in Protonilus Mensae, Mars: Characterization of a water-
834 bearing, energetic gully-forming process, *Earth and Planetary Science Letters*, 294(34),
835 368–377.
- 836 Levy, J., J. W. Head, and D. R. Marchant (2010b), Concentric crater fill in the northern
837 mid-latitudes of Mars: Formation processes and relationships to similar landforms of
838 glacial origin, *Icarus*, 209(2), 390–404.
- 839 Madeleine, J.-B., F. Forget, J. W. Head, B. Levrard, F. Montmessin, and E. Millour
840 (2009), Amazonian northern mid-latitude glaciation on Mars: A proposed climate
841 scenario, *Icarus*, 203(2), 390–405.
- 842 Madeleine, J.-B., J. Head, F. Forget, T. Navarro, E. Millour, A. Spiga, A. Colaitis,
843 A. Määttänen, F. Montmessin, and J. Dickson (2014), Recent Ice Ages on Mars: The
844 role of radiatively active clouds and cloud microphysics, *Geophysical Research Letters*,
845 41(14), 4873–4879.
- 846 Malin, M. C., and K. S. Edgett (2000), Evidence for Recent Groundwater Seepage and
847 Surface Runoff on Mars, *Science*, 288(5475), 2330–2335.
- 848 McEwen, A. S., E. M. Eliason, J. W. Bergstrom, N. T. Bridges, C. J. Hansen, W. A. De-
849 lamere, J. A. Grant, V. C. Gulick, K. E. Herkenhoff, L. Keszthelyi, et al. (2007), Mars
850 reconnaissance orbiter’s high resolution imaging science experiment (HiRISE), *Journal*
851 *of Geophysical Research: Planets*, 112(E5), E05S02.
- 852 Michael, G. G., and G. Neukum (2010), Planetary surface dating from crater size–
853 frequency distribution measurements: Partial resurfacing events and statistical age
854 uncertainty, *Earth and Planetary Science Letters*, 294(3), 223–229.
- 855 Milliken, R., J. Mustard, and D. Goldsby (2003), Viscous flow features on the surface of
856 Mars: Observations from high-resolution Mars Orbiter Camera (MOC) images, *Journal*
857 *of Geophysical Research: Planets (1991–2012)*, 108(E6), 5057.
- 858 Mustard, J. F., C. D. Cooper, and M. K. Rifkin (2001), Evidence for recent climate
859 change on Mars from the identification of youthful near-surface ground ice, *Nature*,
860 412(6845), 411–414.

- 861 Núñez, J., O. Barnouin, S. Murchie, F. Seelos, J. McGovern, K. Seelos, and
862 D. Buczkowski (2016), New insights into gully formation on Mars: Constraints
863 from composition as seen by MRO/CRISM, *Geophysical Research Letters*, doi:
864 10.1002/2016GL068956.
- 865 Okubo, C. H., L. L. Tornabene, and N. L. Lanza (2011), Constraints on mechanisms
866 for the growth of gully alcoves in Gasa crater, Mars, from two-dimensional stability
867 assessments of rock slopes, *Icarus*, 211(1), 207–221.
- 868 Pelletier, J. D., K. J. Kolb, A. S. McEwen, and R. L. Kirk (2008), Recent bright gully
869 deposits on Mars: Wet or dry flow?, *Geology*, 36(3), 211–214.
- 870 Pickett, S. T. (1989), Space-for-time substitution as an alternative to long-term studies, in
871 *Long-term studies in ecology*, pp. 110–135, Springer.
- 872 Pilorget, C., and F. Forget (2016), Formation of gullies on mars by debris flows triggered
873 by co2 sublimation, *Nature Geoscience*, 9(1), 65–69.
- 874 Raack, J., D. Reiss, and H. Hiesinger (2012), Gullies and their relationships to the dust-
875 ice mantle in the northwestern Argyre Basin, Mars, *Icarus*, 219(1), 129–141.
- 876 Reiss, D., S. van Gasselt, G. Neukum, and R. Jaumann (2004), Absolute dune ages and
877 implications for the time of formation of gullies in Nirgal Vallis, Mars, *Journal of*
878 *Geophysical Research: Planets*, 109(E6), E06,007.
- 879 Reiss, D., E. Hauber, H. Hiesinger, R. Jaumann, F. Trauthan, F. Preusker, M. Zanetti,
880 M. Ulrich, A. Johnsson, L. Johansson, et al. (2011), Terrestrial gullies and debris-flow
881 tracks on Svalbard as planetary analogs for Mars, *Geological Society of America Special*
882 *Papers*, 483, 165–175.
- 883 Schon, S. C., and J. W. Head (2011), Keys to gully formation processes on Mars: Relation
884 to climate cycles and sources of meltwater, *Icarus*, 213(1), 428 – 432.
- 885 Schon, S. C., and J. W. Head (2012), Gasa impact crater, Mars: Very young gullies
886 formed from impact into latitude-dependent mantle and debris-covered glacier deposits?,
887 *Icarus*, 218(1), 459–477.
- 888 Schon, S. C., J. W. Head, and C. I. Fassett (2009), Unique chronostratigraphic marker
889 in depositional fan stratigraphy on Mars: Evidence for ca. 1.25 Ma gully activity and
890 surficial meltwater origin, *Geology*, 37, 207–210.
- 891 Schon, S. C., J. W. Head, and C. I. Fassett (2012), Recent high-latitude resurfacing by
892 a climate-related latitude-dependent mantle: Constraining age of emplacement from
893 counts of small craters, *Planetary and Space Science*, 69(1), 49–61.

- 894 Shean, D. E., O. Alexandrov, Z. M. Moratto, B. E. Smith, I. R. Joughin, C. Porter, and
895 P. Morin (2016), An automated, open-source pipeline for mass production of digital
896 elevation models (DEMs) from very-high-resolution commercial stereo satellite imagery,
897 *ISPRS Journal of Photogrammetry and Remote Sensing*, 116, 101–117.
- 898 Smith, I. B., N. E. Putzig, J. W. Holt, and R. J. Phillips (2016), An ice age recorded in
899 the polar deposits of Mars, *Science*, 352(6289), 1075–1078.
- 900 Souness, C., B. Hubbard, R. E. Milliken, and D. Quincey (2012), An inventory and
901 population-scale analysis of martian glacier-like forms, *Icarus*, 217(1), 243–255.
- 902 Squyres, S. W. (1979), The distribution of lobate debris aprons and similar flows on Mars,
903 *Journal of Geophysical Research: Solid Earth*, 84(B14), 8087–8096.
- 904 Treiman, A. H. (2003), Geologic settings of Martian gullies: Implications for their origins,
905 *Journal of Geophysical Research: Planets (1991–2012)*, 108(E4).
- 906 Vincendon, M. (2015), Identification of mars gully activity types associated with ice
907 composition, *Journal of Geophysical Research: Planets*, 120(11), 1859–1879.
- 908 Viola, D., A. S. McEwen, C. M. Dundas, and S. Byrne (2015), Expanded secondary
909 craters in the Arcadia Planitia region, Mars: Evidence for tens of Myr-old shallow
910 subsurface ice, *Icarus*, 248, 190–204.
- 911 Williams, K., O. Toon, J. Heldmann, and M. Mellon (2009), Ancient melting of mid-
912 latitude snowpacks on Mars as a water source for gullies, *Icarus*, 200(2), 418 – 425.